UC Irvine

UC Irvine Electronic Theses and Dissertations

Title

Nicotinic Effect on Auditory Processing: an Unexpected Role of the alpha2 Nicotinic Acetylcholine Receptor

Permalink

https://escholarship.org/uc/item/21s2d79f

Author

Gil, Susan

Publication Date

2021

Peer reviewed|Thesis/dissertation

UNIVERSITY OF CALIFORNIA,
IRVINE

Nicotinic Effect on Auditory Processing:
an Unexpected Role of the alpha2 Nicotinic Acetylcholine Receptor

DISSERTATION

submitted in partial satisfaction of the requirements
for the degree of

DOCTOR OF PHILOSOPHY

in Biological Sciences

by

Susan Gil

Dissertation Committee:
Professor Raju Metherate, Chair
Professor Michael Yassa
Professor Katumi Sumikawa

2021

COPYRIGHT PAGE

DEDICATION

To

my beautiful daughter, Chlöe
The day you were born, you grounded me and gave my life a delightful purpose.

The greatest gift and honor is having you for a daughter.

– Fa Zhou*, Mulan*

Remember your worth.

The flower that blooms in the face of adversity is the rarest and most beautiful of all.

– The Emperor, *Mulan*

TABLE OF CONTENTS

LIST OF FIGURES

LIST OF ABBREVIATIONS

5HT3aR	ionotropic serotonin receptor
α2KO	α2 subunit knockout
α2nAChR	α2 nicotinic acetylcholine receptor
α2eGFP	α2 enhanced green fluorescent protein
A1	primary auditory cortex
ACx	auditory cortex
AP	action potential
BC	basket cell
Chrna2	gene for α2 subunit expression
CN	cochlear nucleus
CF	characteristic frequency
CSD	Current Source Density
dB	decibel
DHβE	dihydro-β-erythroidine
EEG	electroencephalogram
eGFP	enhanced green-fluorescent reporter protein
FS	fast-spiking
IC	inferior colliculi
IHC	immunohistochemistry
KO	knockout
LFP	local field potential
LTP	long-term potentiation
MC	Martinotti cell
MGN	medial geniculate nuclei
MGB	medial geniculate body
nAChR	nicotinic acetylcholine receptor
OL	onset latency
OLM	oriens-lacunosum moleculare
PC	principal cell
PD	postnatal day
PV	parvalbumin

SOC	superior olivary complex
SOM	somatostatin
TAPC	Type-A principal cell
TC	thalamocortical
Th	threshold
VIP	vasoactive intestinal peptide
WT	wild-type

ACKNOWLEDGEMENTS

I would first like to thank my committee chair, Professor Raju Metherate, for reviewing countless drafts, entertaining my countless questions, and offering practical suggestions throughout this process. Above all Raju, thank you for your patience.

I would also like to thank my committee members, Professor Katumi Sumikawa and Professor Michael Yassa. Katumi, your probing questions during committee meetings terrified me, but also forced me to think more critically. Mike, you encourage, support, and push me…and always seem to know at which time each is needed.

Special thanks to my fellow lab members, Irakli Intskirveli, Ronit Lazar, and Dianna Hidalgo for all their help with the tissue preparation, immunolabeling and imaging done for my Chapter 2 experiments. Irakli, I appreciate your training and guidance throughout.

Mike (Dr. Yassa) and Manuella (Dr. Yassa to be), thank you for believing that I am capable, and helping me see that for myself.

Dr. Zavala, I am so very fortunate to be your mentee. In all the years after my graduating from CSULB, you have never failed to check-in on me, and you consistently encourage, teach, advise, support and occasionally talk me off the ledge. I count on your friendship, wit and, of course, your sarcasm. Thanks for everything. I WILL NEVER LEAVE! 😉

To my family and loved ones:

Thank you for your unparalleled love, as well as your continuous support of my pursuing an education, after adulting for so many years. You all have done nothing but encourage me, which has meant more than you know.

A special thanks to Mahreeah. for always raging not only with me, but also on my behalf.

Mami, sin ti este doctorado hubiera sido imposible. Sinceramente, jamás hubiese podido lograr ni siquiera mi licenciatura sin tu apollo, el cual, siempre ha estado centrado en lo mucho que yo se que me quieres. Te agradezco con todo el corazón, tu ayuda, amor, y cariñó. Te adoro.

Turtledove, I owe you my deepest gratitude for your unconditional love and support, as well as your entertaining company. You are my sunshine, mama.

Finally, David Alan. Three years ago, we hadn't met, and now I can't imagine my life without you. Thank you, love, for your gentle yet persistent prompting toward the finish line, and for adding levity, love, and promise to what has been such a trying time. You're my favorite.

CURRICULUM VITAE

EDUCATION

Ph.D.   **Neurobiology and Behavior**, University of California, Irvine, 2021
Dissertation: Nicotinic effect on auditory processing: an unexpected role of alpha2 nicotinic acetylcholine receptor

M.S.   **Neurobiology and Behavior**, University of California, Irvine, 2021

B.S.   **Psychology**, California State University, Long Beach, *magna cum laude*

TEACHING EXPERIENCE AND TRAINING

California Community College Internship Program (2019) –
mentee of Professor Hannah Kang, Orange Coast College

UCI Brain Camp Instructor (2019) - presented workshops and mentored small groups on neuroscience fundamentals (neuroanatomy, neurophysiology, sensory systems, learning and memory, brain dissection, experimental design, conducting experiments, analyzing and interpreting data, poster and symposium presentations), demonstrated experimental techniques

Guest Lecturer for Neuropsychology (2019) - lectured on gateway drugs and drugs of abuse, addiction, and most current related research

Biology of Stress Teaching Assistant (2015-2019) - created exams, graded homework, answered student questions, proctored, graded and input exam scores

Neuropsychology Teaching Assistant (2018) - held office hours, created, graded, and input exam grades

Summer Undergraduate Research Program Writing Mentor (2015-2018) **-** mentored over 20 graduate school-bound students in writing personal statements, statements of purpose, and statements for NSF Graduate Research Fellowship applications

Bio Sci 93 Discussion Section Leader: DNA to Organisms (2015) - attended lectures, prepared and presented lectures for weekly discussion sections, designed and administered quizzes, created and

graded homework assignments, facilitated classroom activities, held office hours, graded exams, attended weekly meetings with faculty and peers

Abnormal Psychology Student Assistant (2013-2014) – held office hours, graded exams

Introduction to Psychology Student Assistant (January 2013-May 2014) - held office hours, graded exams

RESEARCH EXPERIENCE

Department of Neurobiology & Behavior, University of California, Irvine (March 2014-2021)
Auditory Cortex Lab, advisor: Dr. Raju Metherate
- Studied alpha2 nicotinic acetylcholine receptors in auditory cortex
- Trained in *in vivo* local field potential recordings in mouse auditory cortex

Department of Psychology, CSULB – Long Beach, CA (2012 – April 2013)
Developmental Neuropsychopharmacology Lab, advisor: Dr. Arturo Zavala
- Studied effects of pre-weanling methylphenidate administration on rewarding effects of nicotine in adolescent rats
- Trained in breeding and culling litters, administering intraperitoneal and subcutaneous injections, running conditioned place preference sessions

Department of Psychology, CSUSB – San Bernardino, CA (May 2012 – January 2013)
Drug Addiction Lab, advisors: Dr. Cynthia Crawford and Dr. Arturo Zavala
- Studied effects of nicotine exposure on the rewarding effects of methamphetamine.
- Trained in behavioral shaping (rats) and running subjects through long and short access self-administration and extinction sessions; intrajugular catheterization surgeries, in preparation for cocaine/methamphetamine self-administration studies.

FELLOWSHIPS AND AWARDS
- **UC Irvine Center for Hearing Research T32 Training Grant** (2019-2021)
- **UCI Brain Camp Fellowship** (2019)
- **California Community College Internship Program** (2019)
- **National Science Foundation, Graduate Research Fellowship** (2015-2018)

- **UCI Eugene Cota-Robles Fellowship** (2014)
- **UCI Graduate Leading Edge Advancement with Distinction Fellowship** (2014)
- **UCI Diversity Recruitment Fellowship** (2014)
- **UCI Competitive Edge Summer Research Program** (2014)

PUBLICATIONS

Gil, S.M., Metherate, R., (2018). Enhanced Sensory–Cognitive Processing by Activation of Nicotinic Acetylcholine Receptors, *Nicotine & Tobacco Research*.

Pipkin, J.A., Kaplan, G.J., Plant C.P., Bain, S.E., **Gil, S.M.**, Zavala, A.R., Crawford, C.A., (2014). Adolescent and adult nicotine exposure on the acquisition of methamphetamine self-administration and the reinstatement of extinguished methamphetamine-seeking in male rats. *Drug and Alcohol Dependence.*

ABSTRACT OF THE DISSERTATION

Nicotine Effect on Auditory Processing:
an Unexpected Role of the alpha-2 Nicotinic Acetylcholine Receptor

by

Susan Gil

Doctor of Philosophy in Biological Sciences

University of California, Irvine, 2021

Dr. Raju Metherate, Chair

Nicotine enhances cortical neurophysiology and higher cognitive functions, such as attention, learning and memory. This enhancement is presumably mediated by activation of nicotinic acetylcholine receptors (nAChRs), located within central cholinergic systems that mediate attention and other higher brain functions.

Subsequently, nAChR agonists are being considered as prospective therapeutics for treating cognitive disorders. However, the nAChR family is comprised of many subtypes, which differ in composition, expression density, distribution, and nicotinic action. A prudent approach to better inform drug development is to investigate the unique contribution(s) of individual nAChR subtypes to nicotinic cognitive enhancement. Moreover, it is important to consider the possible involvement of less common (and underexamined) nAChR subunits and the role they may play in the overall outcomes of nAChR activation. Using the mouse auditory system, the following experiments explore the physiological role and laminar expression of the alpha2 nicotinic acetylcholine receptor (α2nAChR).

In Chapter 1, I used *in-vivo* electrophysiology within mouse primary auditory cortex (A1), to investigate the role of the underexamined α2nAChR in nicotinic effects on auditory processing. Current-source density recordings within A1 of anesthetized mice revealed that activation of α2nAChRs is involved in the nicotinic enhancement of responses to pure tone stimuli. In fact, compared to wild-type (WT) mice, nicotinic enhancement of A1 responses is altered in mice where the α2 gene has been deleted (α2KO).

In Chapter 2, in order to survey respective laminar distributions, and co-expression within the auditory cortex (ACx), I used immunolabeling of parvalbumin (PV), vasoactive intestinal peptide (VIP), and somatostatin (SOM) interneuron markers on brain sections of mice expressing the enhanced green-fluorescent reporter protein (eGFP). Driven by the α2 promoter, eGFP fluoresced in cells containing the α2nAChR subunit (resulting mice are referred to as α2eGFP mice). We found that α2nAChRs were almost exclusively expressed in Layer V, and generally localized with SOM-expressing interneurons.

Together these chapters represent the initial physiological and anatomical investigations of α2nAChRs in the ACx. They serve to further our understanding of α2nAChRs function in auditory processing.

INTRODUCTION

Auditory system

Like the visual and somatosensory systems, the auditory system is topographically organized. However, while topographic layouts of visual and somatosensory systems correspond to physical locations within our environment, the same does not apply to the auditory system. Instead, all auditory stimuli (i.e., sound waves) make their way to the inner ear, activating the basilar membrane, which produces the downstream topographic organization of neurons, by frequency (Pickles, J.O., 2015; Wu et al., 2015). This topographic representation is then relayed through the ascending pathway.

Auditory stimuli begin as vibrations at various frequencies that displace air, causing changes in air pressure that reach the outer ear (pinna). The eardrum preserves these frequencies and transforms the changes in air pressure into vibrations that travel through the middle ear, to the inner ear. There, vibrations are converted into hydraulic energy, and then transduced into neurochemical signals that enter the brain via the cochlear nerve. Within the brain, these signals are relayed through subcortical structures to the auditory cortex within the temporal lobe. The information is carried through excitatory and inhibitory signals, mediated by activation of various receptor types expressed by neuronal circuitry. Signals arrive at the cochlear nucleus (CN) within the brainstem. Contra- and ipsilateral CN projections innervate the superior olivary complex (SOC), which sends projections to the nucleus of lateral lemniscus. Efferent fibers project from the lateral lemniscus to the inferior colliculi (IC). These neurons

1

project to the medial geniculate body (MGB) within the thalamus, and the ventral portion

of MGB (the MGv), sends tonotopic information to the primary auditory cortex (A1)

(Pickles, J.O., 2015; Wu et al., 2015). See Figure 1.

Figure 1: Ascending auditory pathway. The cochlea houses the basilar membrane, which is organized tonotopically. Stimulation of the basilar membrane is transduced into neurochemical signals which are relayed by cascading regions (CN →SOC → IC → MGB → ACx) of the ascending auditory pathway. This tonotopic information is sent to A1 within auditory cortex (Patterson et al., 1999), adapted.

Spectral integration

The task of integrating incoming frequency-related neural information within A1

(i.e., spectral integration) involves the interconnecting of frequency representations to

allow for processing of spectrally complex stimuli (Metherate et al., 2005), such as

vocalizations in animals and speech in humans. Spectral integration results in receptive

fields, in which the centers reflect responses elicited by stimuli at characteristic

frequency (CF). The surrounding portions reflect weaker responses elicited by nonCF

stimuli. Although extracellular recordings indicate a relatively constant breadth of

suprathreshold frequency receptive fields (i.e., those based on action potential

recordings) throughout the main (lemniscal) ascending auditory pathways (Calford et

2

al., 1983), other studies use intracellular recordings to show that single neurons within A1 receive subthreshold inputs across a much broader range of frequencies (Kaur et al., 2004; Intskirveli and Metherate, 2012; Metherate et al., 2005). It is hypothesized that integration of bottom-up (thalamocortical) spectral inputs within A1 is accomplished via intracortical processing, modulated (top-down) by behavioral state (e.g., sleep, waking, and attention) and experience (Metherate et al., 2005). Importantly, it is thought that the mechanism behind this modulation is, in part, the activation of nAChRs (so named because of their affinity to nicotine). These receptors are of special interest because they play important roles in the regulation of cognition. Thus, as nAChRs are involved in mediating sensitivity to both bottom-up sensory information and top–down regulation from higher cortical regions, a detailed understanding of nicotinic modulation, including the location and function of relevant nAChR subtypes, is central to understanding the circuitry involved in various cognitive processes.

nAChR regulation of cognitive and cortical functions

Nicotine enhances sensory–cognitive functions via nAChRs that also are activated by attention-related release of the endogenous neurotransmitter, acetylcholine. Performance on sensory-related tasks is improved by nicotine and, conversely, impaired by nicotinic antagonists, genetic deletion of nAChRs, or disease-induced loss of nAChRs (Warburton, 1992; Terry et al., 1996; Evans and Drobes, 2009; Sarter and Howe, 2009; Levin et al., 2006; Horst et al., 2012). Similarly, for decades it has been known that nicotine enhances cognitive and cortical functions more broadly,
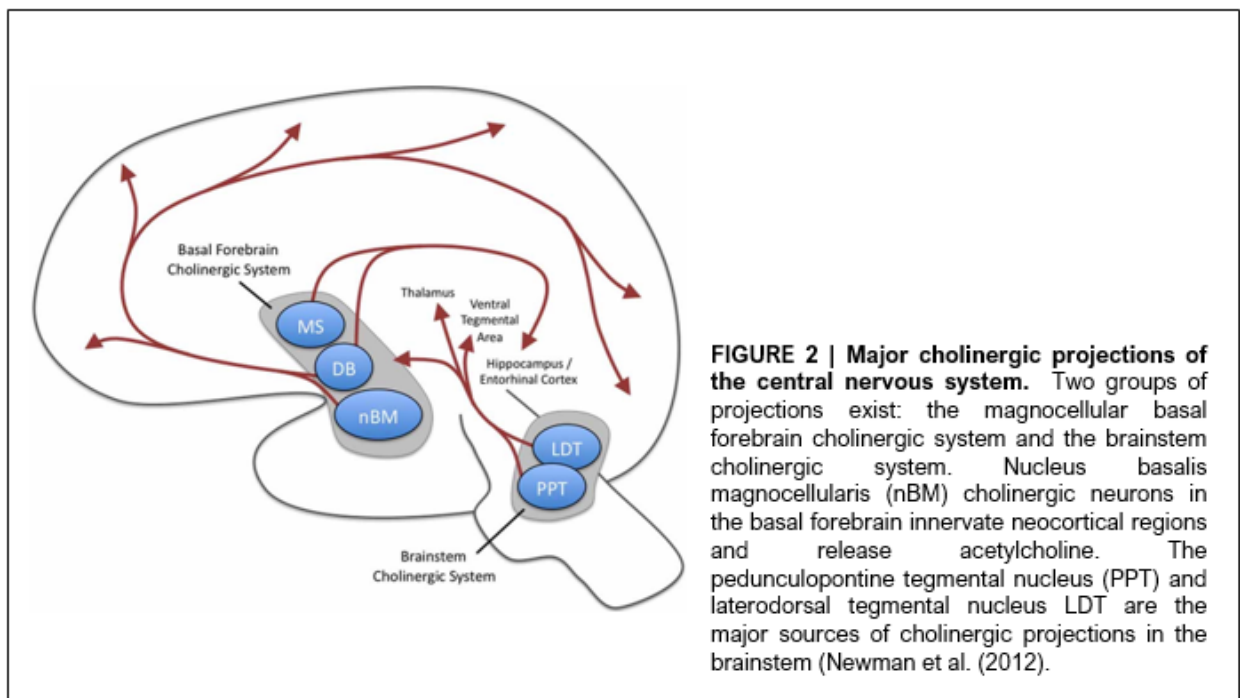
as evidenced by studies that focus on, for example, learning and memory, attention, and cortical neurophysiology (Terry et al., 1996; Evans and Drobes, 2009; Sarter and Howe, 2009; Grilly, 2000; Newhouse P et al., 2012). In animal models, systemic nicotine enhances working memory, reference memory, memory acquisition, memory restitution, and associative learning (Levin et al., 2006; French et al., 2006; Arendash et al., 1995; Riekkinen et al., 1997; Socci et al., 1995). Attention-related studies, such as those that measure readiness to detect brief sensory signals at unpredictable intervals, also reveal increased accuracy with nicotine (Grilly, 2000).

Results of human studies on smokers also indicate enhanced performance in cognition, for example, in visual information processing (Lawrence et al., 2002). Although enhanced performance in smokers can be partly attributed to relief from nicotine withdrawal (induced by abstinence before testing), studies show enhanced function in nonsmokers as well (Levin et al., 2006). In human subjects, including both smokers and nonsmokers, nicotine (e.g., via transdermal patch) can improve working memory (Levin et al., 2006).

Nicotine also affects cortical neurophysiology in a manner consistent with enhanced cognition. For example, in electroencephalogram studies nicotine increases spectral power at electroencephalogram (EEG) frequencies associated with arousal, while decreasing power at EEG frequencies associated with a relaxed state (Mansvelder et al., 2006). Similarly, in studies utilizing functional magnetic resonance imaging, nicotine increases activation of frontal networks during attention-related tasks (Mansvelder et al., 2006). Thus, physiological and behavioral studies consistently show

that nicotine can enhance sensory–cognitive function.

It is generally assumed that the pro-cognitive effects of nicotine depend on activating nAChRs associated with central cholinergic systems that mediate attention and other higher brain functions (Crooks et al., 2014). Nucleus basalis cholinergic neurons in the basal forebrain innervate neocortical regions and release acetylcholine (Figure 2), which binds to cortical nAChRs (and muscarinic acetylcholine receptors), enhancing cortical function (Wenk GL, 1997).

FIGURE 2 | Major cholinergic projections of the central nervous system. Two groups of projections exist: the magnocellular basal forebrain cholinergic system and the brainstem cholinergic system. Nucleus basalis magnocellularis (nBM) cholinergic neurons in the basal forebrain innervate neocortical regions and release acetylcholine. The pedunculopontine tegmental nucleus (PPT) and laterodorsal tegmental nucleus LDT are the major sources of cholinergic projections in the brainstem (Newman et al. (2012).

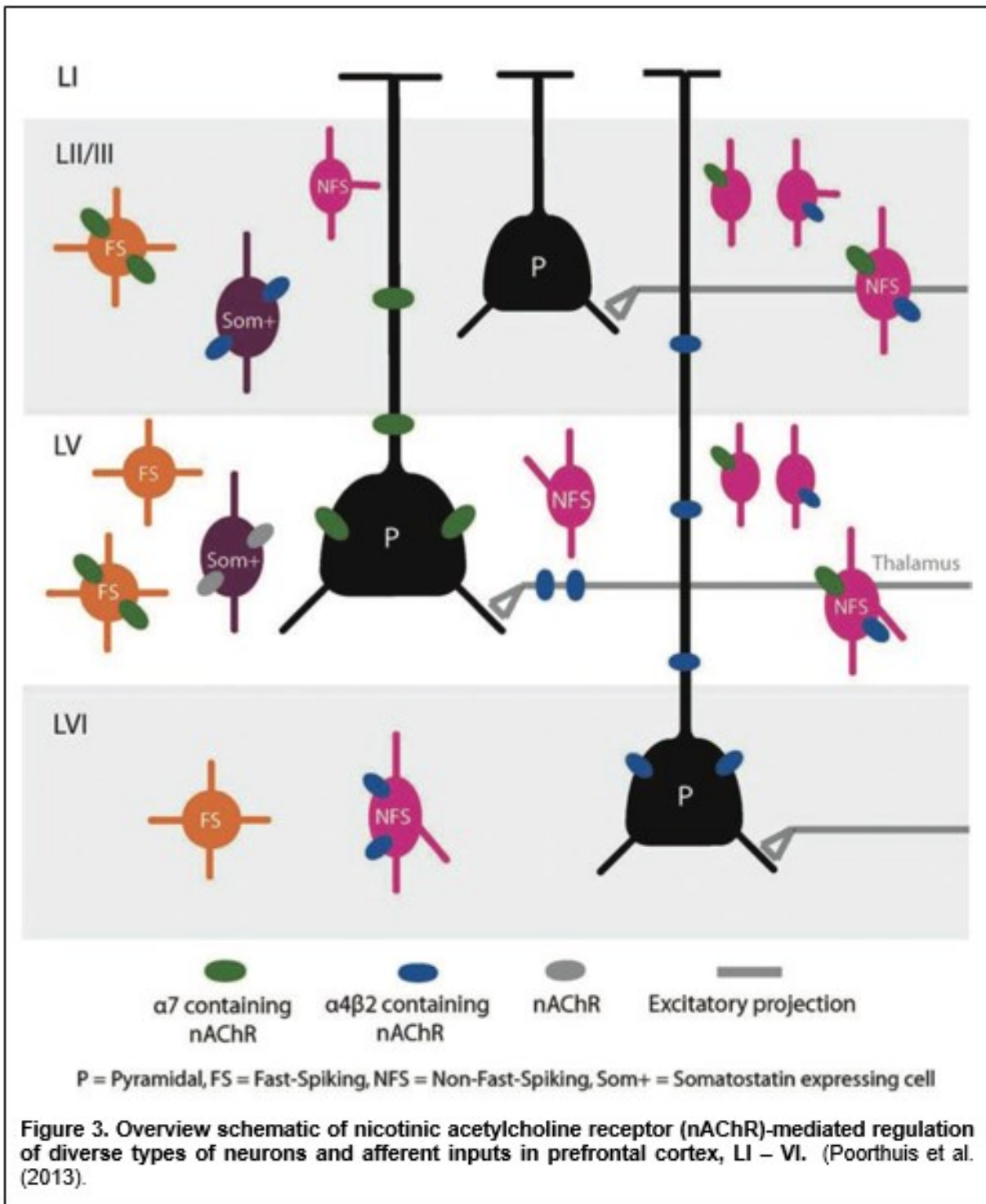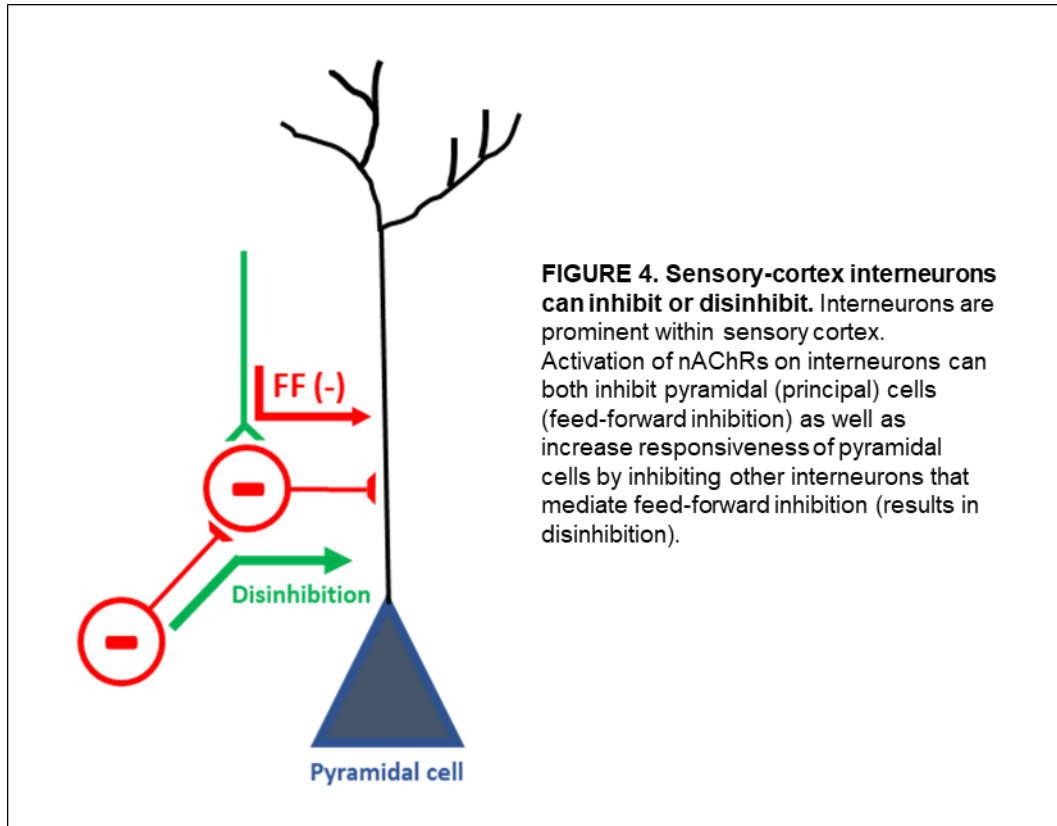In sensory as well as non-sensory cortex, nAChRs are found presynaptically on terminals of both excitatory and inhibitory neurons, including, in some cases, the terminals of thalamocortical projection neurons (Figure 3) (Poorthuis et al., 2013; Kawai et al., 2007; Gil et al., 1997; Aracri et al., 2010). Activation of presynaptic nAChRs on axon terminals can enhance synaptic transmission by increasing neurotransmitter

release (McGehee et al., 1995; Girod R et al., 2000). Enhanced sensory thalamocortical transmission also may involve nAChRs located in the subcortical white matter, where they act to enhance the speed and synchrony of axonal propagation (Kawai et al., 2007; Mukherjee et al., 2018; Askew et al., 2017). Postsynaptic nAChRs also occur throughout cortex and act to increase excitability (Poorthuis et al., 2013; Albuquerque et al., 2009; Pi et al., 2013; Porter et al., 1999; Poorthuis et al., 2013).

However, actions of nAChRs to excite inhibitory interneurons are particularly prominent in studies of the hippocampus and sensory cortices, where they can directly inhibit principal cells (PCs) as well as indirectly increase their responsiveness by inhibiting other interneurons that mediate feed-forward inhibition (Albuquerque et al., 2009; Pi et al., 2013; Porter et al., 2013; Takesian et al., 2004), as depicted in Figure 4.

Thus, nAChRs can be presynaptic, postsynaptic, and axonal; and located on both excitatory and inhibitory neurons (Figure 3).   Understanding how diverse nicotinic actions integrate to enhance cortical and cognitive functions is a notable challenge in current research.

Figure 3. Overview schematic of nicotinic acetylcholine receptor (nAChR)-mediated regulation of diverse types of neurons and afferent inputs in prefrontal cortex, LI – VI. (Poorthuis et al. (2013).

FIGURE 4. Sensory-cortex interneurons can inhibit or disinhibit. Interneurons are prominent within sensory cortex. Activation of nAChRs on interneurons can both inhibit pyramidal (principal) cells (feed-forward inhibition) as well as increase responsiveness of pyramidal cells by inhibiting other interneurons that mediate feed-forward inhibition (results in disinhibition).

Therapeutic properties of nAChR activation

Because activation of nAChRs enhances cognitive functions generally, nicotinic agonists (including nicotine itself) are being tested as potential therapeutic treatments for cognitive disorders in adults, especially those that involve diminished attention, learning, and memory (Crooks et al., 2014; Newhouse PA et al., 2004; Gold et al., 2012; Potter and Newhouse, 2008). In patients with Alzheimer's disease, nicotine and related agents improve cognitive outcomes, including the acquisition and retention of visual and verbal information, decreased errors, and improved performance on cognitively demanding tasks (Newhouse P et al., 2012; Newhouse PA et al., 2004). For adults with attention deficit disorders, nicotinic agonists moderately improve symptoms (Levin et al.,

2006; Potter and Newhouse, 2008). In patients with schizophrenia, nicotine improves cognitive functioning such as spatial processing in smokers, and attention in both smoking and non-smoking patients (Levin et al., 2006; Newhouse PA et al., 2004).
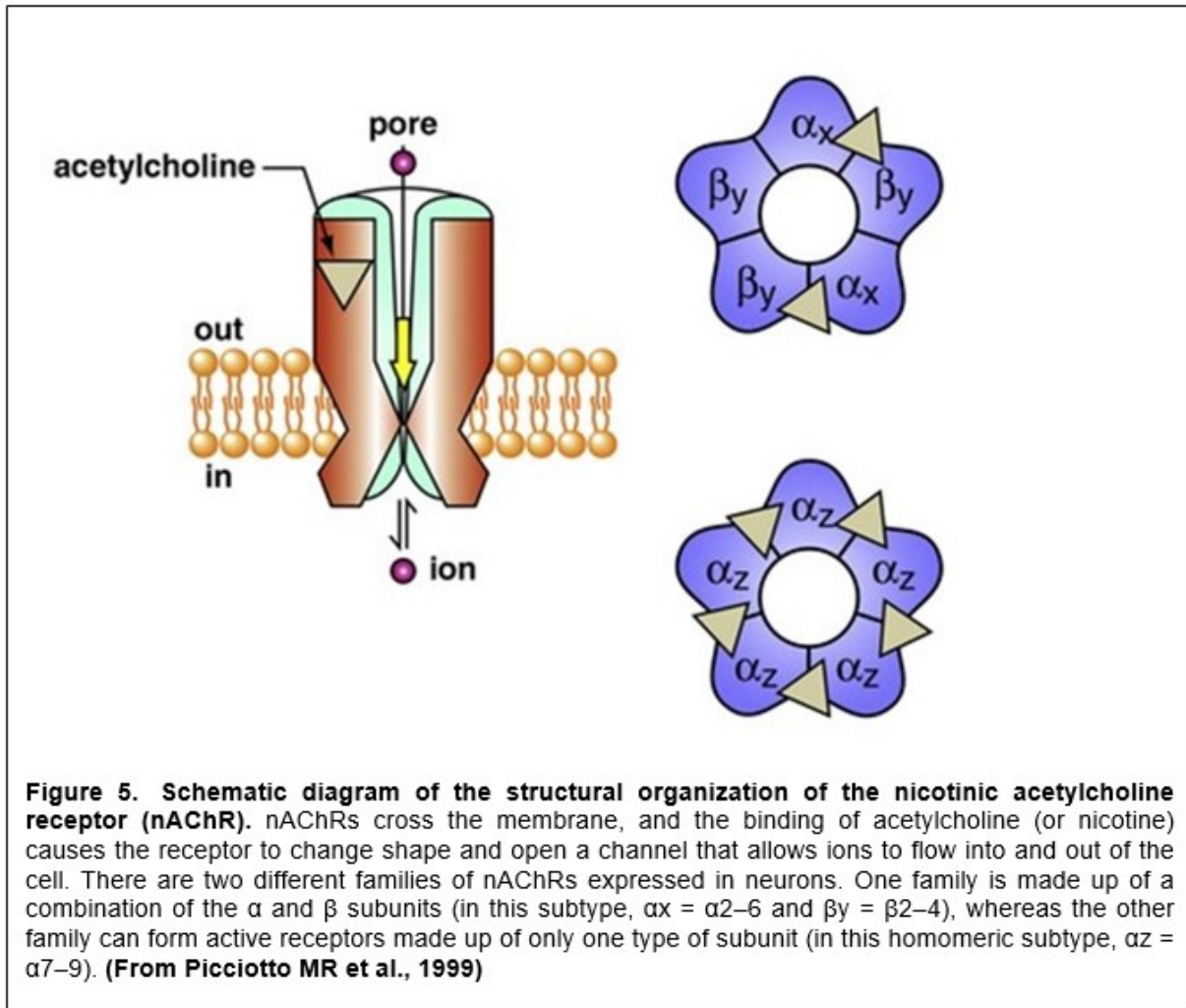
A potential therapeutic for enhancing cognition is the use of transdermal patches or gum. Although this naturally raises concerns about potential misuse/abuse, remission, and addiction liability, existing evidence suggests that nicotine, when delivered topically (patch) or orally (gum), does not lead to dependence, as few people use nicotine gum for non-cessation purposes (Hughes et al., 2004). However, the best approach to address addiction liability of nicotine replacement therapy is to test its long-term administration on nonsmoking participants. In a study by Newhouse et al. (2012), nonsmoking elderly adults with mild cognitive impairment were administered 15 mg/day of nicotine via transdermal patch over a period of 6 months. After completion of the study, none of the participants experienced withdrawal symptoms, and none continued nicotine use (Newhouse P et al., 2012). Also important for long-term use, nicotine's efficacy for improving memory does not decrease over time (Levin et al., 2006). These results highlight the promise of nicotinic agents as therapeutics and the importance of developing agents that do not lead to dependence and other adverse side effects. Optimization of nicotinic treatments for cognitive disorders, including the use of subtype-specific nicotinic agonists (Taly et al., 2009), requires comprehensive knowledge of nAChR composition and distribution, and an understanding of their integrated effects on neural systems.

Nicotinic acetylcholine receptor structure and function

Nicotinic acetylcholine receptors are the prototypic ionotropic receptor. Besides nicotine, they bind endogenous acetylcholine (Albuquerque et al., 2009; Dani and Bertrand, 2007). These receptors comprise five subunits arranged around a pore that functions as an ion channel (Figure 5). Neuronal subtypes of nAChRs are either homomeric with five α subunits or heteromeric with a combination of α and β subunits from two sub-families, α2 through α10 and β2 through β4 (Albuquerque et al., 2009; Dani and Bertrand, 2007; Ortells and Barrantes, 2010). Together, studies expressing nAChRs in *Xenopus oocytes* have identified the effects of different α/β subunit combinations on receptor function, including channel kinetics and ion permeability, notably to Ca^{2+} (Albuquerque et al., 2009; Dani and Bertrand, 2007; Mazzaferro et al., 2017).

The predominant subtypes in the brain are homomeric α7 nAChRs, which have low affinity for nicotine, and heteromeric α4β2* nAChRs that bind nicotine with high affinity (the asterisk represents possible additional, accessory subunits that can alter function (Albuquerque et al., 2009; Dani

and Bertrand, 2007; Mazzaferro et al., 2017). Together, they comprise 90% of nAChRs in the cerebral cortex (Wada et al., 1989; Mao et al., 2008). Additional subunits such as α2 are found in cortex at low levels (Wada et al., 1989; Mao et al., 2008) likely contribute critically to certain functions (Xiao and Kellar, 2004).

The diversity of nAChR function conferred by receptor location (pre- and postsynaptic; excitatory and inhibitory neurons), is multiplied by the array of nAChR

Figure 5. Schematic diagram of the structural organization of the nicotinic acetylcholine receptor (nAChR). nAChRs cross the membrane, and the binding of acetylcholine (or nicotine) causes the receptor to change shape and open a channel that allows ions to flow into and out of the cell. There are two different families of nAChRs expressed in neurons. One family is made up of a combination of the α and β subunits (in this subtype, αx = α2–6 and βy = β2–4), whereas the other family can form active receptors made up of only one type of subunit (in this homomeric subtype, αz = α7–9). **(From Picciotto MR et al., 1999)**

subtypes. This complexity is represented in Figure 3, which depicts locations and subunit composition of nAChRs in prefrontal cortex (Poorthuis et al., 2013). Additional characteristics of nAChRs that affect synaptic transmission and modulation are receptor desensitization (decreased response in the continued presence of agonist), and upregulation (increased receptor number after chronic exposure to agonist) (Ortells and Barrantes, 2010). Thus, a full understanding of therapeutic nicotinic regulation will require integrating the contributions of diverse nAChRs with varying subunit composition, distribution, and response to chronic use of agonist.

11

Functions of nicotinic acetylcholine receptors in auditory cortex

Activation of nAChRs is known to enhance sensory–cognitive function in auditory (and other sensory) (Warburton, 1992; Levin et al., 2006). Performance on auditory tasks is improved by nicotine and, conversely, impaired by nicotinic antagonists, genetic deletion of nAChRs, or disease-induced loss of nAChRs (Warburton, 1992; Terry et al., 1996; Evans and Drobes, 2009; Sarter and Howe, 2009; Levin et al., 2006; Horst et al., 2012). Although the precise functions regulated by nAChRs are not fully understood, it is useful to consider nicotinic regulation of auditory–cognitive function within a framework of spectral integration of afferent inputs to primary auditory cortex (A1). A recurring hypothesis is that nicotine improves "attentional narrowing" to focus attention on relevant acoustic stimuli, including speech (Trimmel and Wittberger, 2004; Friedman et al., 1974; Knott et al., 2009; Kassel, 1997). In auditory cortex, systemic nicotine enhances neural processing, producing narrower receptive fields, with increased gain (Askew et al., 2017; Intskirveli and Metherate, 2012; Kawai et al., 2011) (Figure 6). This effect mimics that of auditory selective attention (Okamoto et al., 2007; O'Connell et al., 2014; Lakatos et al., 2013), likely because nicotine activates nAChRs normally activated by top-down influences on spectral integration. This activation likely contributes to nicotine-induced auditory-cognitive enhancement.

Although nicotine is delivered systemically, the locus of excitatory action is within A1 and the auditory thalamocortical pathway, as the excitatory effects of systemic nicotine are blocked by local injection of the antagonist dihydro-β-erythroidine (DHβE) and mimicked by local injection of agonist or a positive allosteric modulator (Askew et al.,

Figure 6. Systemic nicotine enhances gain and narrows receptive fields in mouse A1. Left: Example traces are current sinks in Layer IV of anesthetized mice, recorded using a 16-channel linear probe and evoked by acoustic "notched-noise" stimuli centered at the characteristic frequency (CF) (i.e., white noise filtered to remove a spectral "notch" centered at CF for the recording site). Current sinks reflect stimulus-evoked synaptic activity at the recording site. Example shows that a narrow-notch stimulus that activates most of the receptive field produces a robust current sink (top black trace) that is enhanced by systemic nicotine (2 mg/kg), indicating increased gain. A wide-notch stimulus that activates only the edges of the receptive field produces a weaker response that is abolished by nicotine (bottom), indicating narrowing of the receptive field by nicotine. Right: group data from current-source density recordings in 23 mice plotting the initial slope of Layer-IV current sink versus notch width of stimulus (normalized to a reference width that elicits the half-max response in each animal). Systemic nicotine enhances gain (curve shifts to higher values) and narrows receptive fields (curve shifts to narrower notch widths). Modified from Askew et al. (2017).

2017; Intskirveli and Metherate, 2012; Kawai et al., 2011). Inhibitory effects of systemic nicotine also are seen in A1, as well as in the auditory midbrain and thalamus (Askew et al., 2017). It is important to note that, although historically the effects of DHβE have been interpreted as implicating α4β2* nAChRs, given their predominance in cortex, DHβE also binds to α2β2 nAChRs (Xiao and Kellar, 2004), and their contributions cannot be precluded. Potential functional consequences of nAChRs containing α2 subunits will be discussed next.

Potential contributions to cortical function of α2-containing nAChRs

Recently, several studies have suggested a role in cortical function for nAChRs containing α2 subunits, serving to emphasize the possibility that even nAChR subunits that are relatively sparse (<3% of cortical nAChR subunits for α2 (Mao et al., 2008)) may play an important functional role (Whiteaker et al., 2009). Historically, the α2 subunit was among the first neuronal nAChR subunits studied in co-expression with β2 subunits (Whiteaker et al., 2009). However, because of its relatively low levels in cortex and the pharmacological properties it shares with the ubiquitous α4 subunit, most studies have focused on the latter (Whiteaker et al., 2009). Both α2 and α4 subunits are agonist-binding subunits that form functional receptors with β2 subunits (Wada et al., 1988). In comparing α2 and α4 subunits, several differences emerge (Wada et al., 1989; Wada et al., 1988). Whereas α4 subunits are expressed in all cortical layers and in hippocampus, α2 subunit expression is the most restricted (in rodent) and is selectively expressed in cortical Layers V and VI, and in a subpopulation of hippocampal interneurons (OLM interneurons). Although α2nAChRs are expressed sparsely (in rodent), it is important to note that they appear to be highly expressed in all layers of nonhuman primate cortex (Han et al., 2000) and in human cortex (Gotti et al., 2006), leading to the speculation that evolutionary pressure has resulted in increased expression of α2 nAChRs in cortex (Han et al., 2000).

Recent studies in mouse have revealed an important role for α2 subunit-expressing interneurons in hippocampal function, specifically, long-term potentiation (LTP), a putative cellular mechanism of learning and memory (Nakauchi et al., 2007; Jia

et al., 2009; Kleeman et al., 2016; Lotfipour et al., 2017). In hippocampal slices, whole-cell recordings show that presumed OLM interneurons discharge continuously (without desensitization) during application of nicotine, and single-cell reverse transcription-polymerase chain reaction analysis indicates that these cells express α2 subunits (Jia et al., 2009). The results suggest that sustained activation of α2 nAChRs produces continuous firing of OLM interneurons (Jia et al., 2009). These α2 nAChR-expressing interneurons regulate the production of LTP (Nakauchi et al., 2007; Leão et al. 2012). Nicotinic facilitation of LTP in the Schaffer collateral input to CA1 is abolished in mutant mice lacking α2 nAChRs (Nakauchi et al., 2007) and enhanced in mice with "hypersensitive" α2 nAChRs (serine for leucine substitution resulting in 100-fold increased sensitivity) (Lotfipour et al., 2017). Similarly, optogenetic activation of α2 nAChR-expressing neurons enhances LTP, whereas loss of α2 nAChR-mediated function abolishes nicotinic enhancement of LTP (Leão et al. 2012). Additionally, behavioral studies show that genetic deletion of α2 nAChRs impairs hippocampal-dependent spatial memory (Kleeman et al., 2016).

These recent studies: 1) indicate that even the sparsely expressed α2nAChR may play an important role in nicotinic regulation of cortical function; and 2) suggest it may be useful to target these subunits via loss of function studies within A1, in order to isolate α2nAChRs contribution to nicotinic enhancement of auditory cognition.

However, potential combinations of subunits (α2-α10 and β2-β4) result in a diverse set of pentameric ion channels (i.e., distinct nicotinic targets) and diverse effects of nicotine, since subunit combination, as well as expression density and distribution all

contribute to ultimately determining nicotinic action. With $\alpha4\beta2$ and $\alpha7$ subtypes comprising 90% of cortical nAChRs, drug development has focused on selectively targeting these receptors. Yet, success has been limited, emphasizing that there are still many unknowns regarding nAChR subtypes and their respective functions and possible interactions within cortical processing. A prudent approach is to investigate the unique contribution(s) of individual nAChR subtypes to nicotinic cognitive enhancement, to better inform drug development. Moreover, it is important to consider the possible involvement of less common (and underexamined) nAChR subunits and the parts they may play in the overall behavioral outcomes of nicotine administration. In both human and rodent behavioral studies, nicotinic enhancement is more evident in performance on complex tasks (Levin et al., 2011). However, it is unclear which nAChR(s) mediate this enhancement. In regard to rarer nAChR candidates, the $\alpha2$ subunit containing nAChR (3% of cortical nAChRs) has recently garnered attention, as $\alpha2$ subunit-containing oriens-lacunosum moleculare (OLM) interneurons (a subset of somatostatin (SOM)-expressing interneuron population) have been shown to play a critical role in hippocampal processing, specifically in nicotine-enhanced long-term potentiation (Nakauchi et al., 2007; Lotfipour et al., 2017). However, the $\alpha2$ nAChR's role in cortical processing, specifically auditory processing, is not known. Characterization of $\alpha2$nAChR-mediated effects within the context of auditory processing is an important step toward understanding how particular behaviors are mediated by activation of distinct nAChR subtypes. Moreover, studying under-investigated, sparsely expressed nAChR subtypes such as the $\alpha2$nAChR affords us the opportunity to build on our
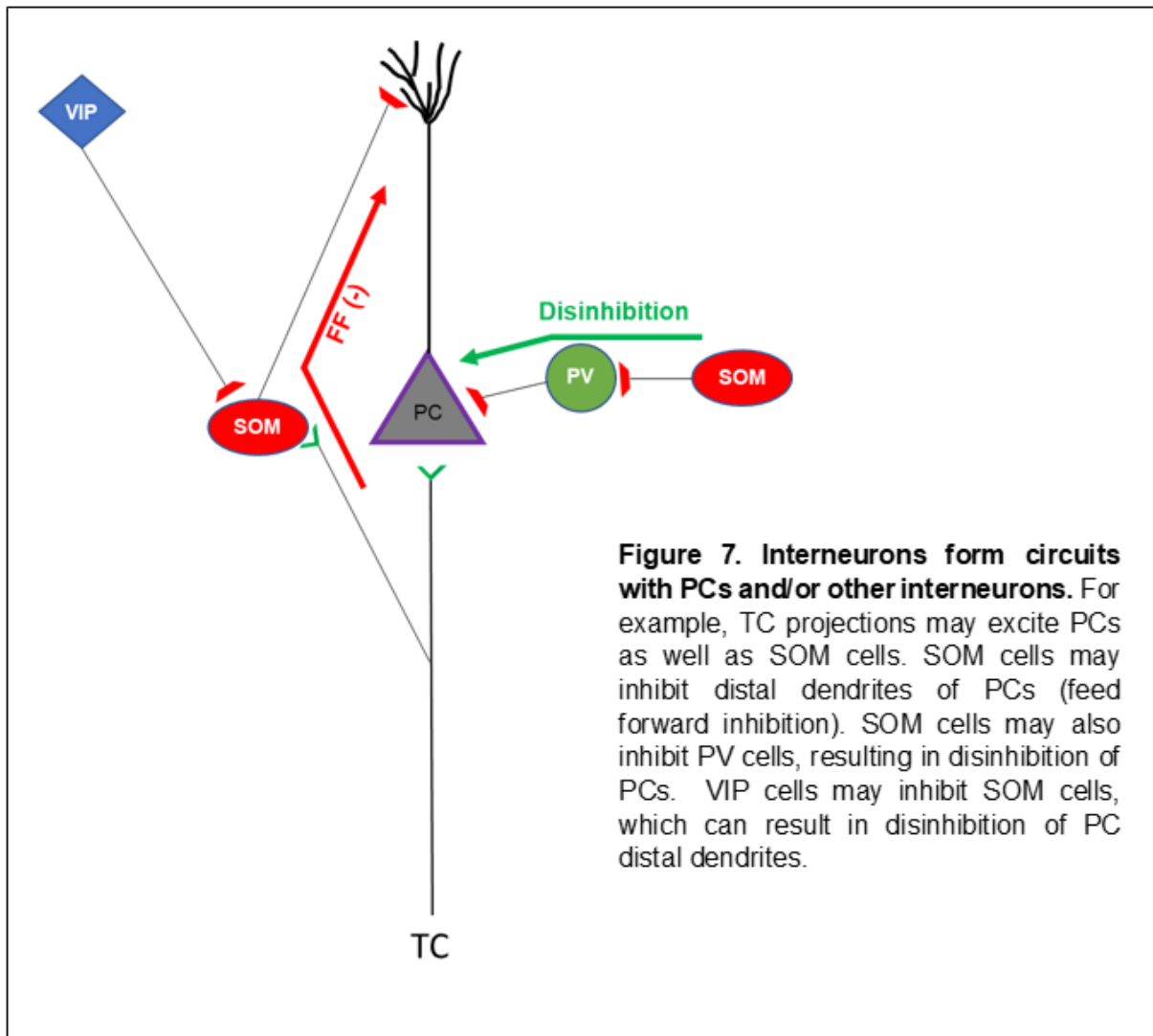
16

fragmented understanding of neuronal circuitry within the neocortex. Chapter 1 of this dissertation provides the important, first stepping-stone in understanding the significant role α2nAChRs play in auditory processing of pure tones.

Cortical Interneurons

Processing and responding to sensory stimuli require dynamic and flexible interactions between excitatory and inhibitory neural activity, which is generally carried out by (glutamatergic) PCs and local (GABAergic) interneurons, respectively (Scheyltjens and Arckens, 2016; Shigematsu et al., 2019). Orchestrated exchanges between these primary players give rise to complex patterns of brain activity fundamental not only to sensory processing but other cognitive functions such as attention, learning and memory (Rudy et al., 2011). In the auditory system, inhibitory systems are important for temporal precision. Interneurons provide GABAergic modulation of excitatory inputs, crucial for controlling information flow, oscillatory behavior, and runaway excitation (Rudy et al., 2011; Griguoli and Cherubini, 2012). Disruptions in normal interneuron function have been implicated in disorders such as schizophrenia, autism, and epilepsy (Goldberg and Coulter, 2013; Volk and Lewis, 2014; Marin, 2012).

Surprisingly, considering their extensive influences, interneurons make up only 10-20% (rodents) of all cortical neurons (Rudy et al., 2011). They are present in all cortical layers where they form circuits with PCs and/or other interneurons (Figure 7). They are a highly diverse cell population, and laminar expression, morphology, intrinsic

membrane properties, firing patterns, and synaptic inputs and targets can vary, depending on the interneuron class and subtype (Rudy et al., 2011; Tremblay et al., 2016). Many of these attributes have also served as ways in which to classify interneurons. One way to categorize interneurons is by their respective expression of non-overlapping molecular markers: PV (Ca^{++}-binding protein), the ionotropic serotonin receptor (5HT3aR), and SOM (neuropeptide). This scheme accounts for nearly 100% of GABAergic interneurons (Rudy et al., 2011).

Figure 7. Interneurons form circuits with PCs and/or other interneurons. For example, TC projections may excite PCs as well as SOM cells. SOM cells may inhibit distal dendrites of PCs (feed forward inhibition). SOM cells may also inhibit PV cells, resulting in disinhibition of PCs. VIP cells may inhibit SOM cells, which can result in disinhibition of PC distal dendrites.

If we consider only PV, VIP (sub-type of 5HT3aR class), and SOM -expressing interneurons, we include the three most highly expressed subtypes and 82% of all cortical interneurons. Using immunohistochemistry, staining protocols, and electrophysiology on transgenic mouse lines (fluorescent labeling) allows us to study their laminar expression, morphology, and physiological properties (respectively) (Jiang et al., 2015, Riedemann, 2019).

PV-expressing interneurons comprise 40-50% of all interneurons, making it the largest class within the neocortex (Riedemann, 2019, Rudy et al., 2011). All are fast-spiking cells (FS), meaning that they fire sustained high-frequency trains of brief action potentials (AP), with little spike frequency adaptation (Tremblay et al., 2016). They also exhibit fast after hyperpolarization – usually generated by single action potentials. PV cells are the dominant inhibitory system in the neocortex, comprised of two main morphologies -- basket and chandelier cells; both are distributed throughout laminae, except for Layer I (Rudy et al., 2011). Their axonal and dendritic architecture vary across cortical layers. For example, axons and dendrites of Layer-IV PV cells remain local, but some Layer-V PV cells have local and translaminar axons (Reidemann, 2019).

Basket cells (BC) are the main thalamocortical targets in Layer IV, mediating feedforward inhibition of thalamocortical sensory responses in PCs. In addition, they exert powerful perisomatic inhibition within cortical circuits, highly impacting the output of their targets and surrounding cells, demonstrated by Packer and Yuste (2011). Using paired recordings, they discovered that a given BC contacts a majority of its surrounding pyramidal cells.

Many BCs have expansive dendrites that extend across laminae, which allows them to integrate input from PCs both locally and from multiple layers (Hu et al., 2014). Moreover, their dendrites are connected by gap junctions, which also allows them to share excitatory input. Together these characteristics BCs to mediate both feedforward and feedback inhibition. In addition, dendritic properties of BCs result in a high threshold for activation. Once they reach threshold, they activate and deactivate very quickly. This provides for precisely timed APs from BCs, enabling them to establish and maintain gamma frequency cortical rhythms, which are associated with attention, memory, and plasticity (Rudy et al., 2011).

Precisely timed feedforward inhibition means that temporal summation of excitatory inputs to PCs must occur within a very small time-window (Hu et al., 2012). These characteristics ensure that APs within PCs are also triggered with temporal precision. Regarding feedback inhibition, the reciprocal inputs between BCs and PCs mediate a "winner-takes-all" dynamic (Hu et al., 2012). In this scenario, as the PC is activated, it in turn activates the BC, whose inhibitory effects creates the small temporal window discussed above. Only PCs with the strongest inputs can overcome this temporal parameter to achieve APs; surrounding cells remain inhibited (Hu et al., 2012). BCs also play a role in cortical disinhibitory circuits, where they are the target of inhibition by VIP and SOM interneurons.

Chandelier cells (the other PV cells) are most dense at the border of Layers I and II, but also expressed in Layer V/VI. They mainly target the axon initial segment of

pyramidal cells (Figure 7). While basket cells are more common in sensory cortices, chandelier cells are expressed more in frontal cortices Tremblay et al., 2016).

VIP interneurons are classified based on their expression of vasoactive intestinal peptide, which as the name implies, was first discovered in the intestine (Said and Mutt, 1970). Its presence was later discovered in a class of cortical interneurons expressed in many brain regions (Rudy et al., 2011; Xu and Callaway, 2009). VIP cells comprise 40% of the 5HT3a interneuron class, which all express the 5HT3a receptor (Ferezou et al., 2002). It is worth noting that VIP cells express nAChRs (Fu et al., 2014). VIP expression is most dense in Layer II/III. The two main morphologies for VIP cells are bipolar, and multipolar.

Bipolar cells account for 50% of VIP interneurons. They are also referred to as irregular-spiking cells, which describes their firing patterns when near threshold (Rudy et al., 2011). During larger depolarizations, however, they have a repetitive firing pattern (Porter et al., 1998). Bipolar cells are highly excitable, due to their high input resistance, and target mostly SOM interneurons (Tremblay et al., 2016). See Figure 7.

The SOM-expressing class of interneurons is off special interest in this dissertation, as one of its sub-types has been shown to express the α2nAChRs (Lotfipour et al., 2017; Leao et al. 2012). SOM interneurons make up 30% of cortical interneurons and are expressed in all layers except Layer I. This class of interneurons targets mainly distal dendrites of PCs (Figure 7). Sixty-six percent of SOM cells are electrically coupled by dendritic gap junctions, which increase efficiency at relaying chemical signals and affect networks in a location specific manner (Timofeeva et al.,

2013). The electrophysiological properties of SOM cells are different from those of PV and VIP interneurons, in that SOM cell membranes are more depolarized and have higher rectification of hyperpolarizing pulses (Riedemann, 2019). In addition, when compared to PV cells, SOM cells have slower spike kinetics. Except for those expressed in supragranular layers, SOM cells are also known as low-threshold spiking (LTS) because they exhibit low-threshold calcium spikes (Riedemann, 2019, Mao et al., 2003). This occurs when low volage-activated T-type calcium channels open in response to small membrane depolarizations and allow calcium into the cell, during a hyperpolarized state. These channels deactivate quickly, but their influence can depolarize cells until they reach threshold, and canonical high-voltage calcium channels open (Cain and Snutch, 2013). Most SOM cells display a regular discharge pattern with frequency adaptation. Remaining cells display a stuttering firing pattern and almost no frequency adaptation, resembling FS PV cells.

There are two main classes of SOM cells – Martinotti cells (MCs), and non-Martinotti cells. Non-Martinotti cells are the smaller fraction of SOM cells, and include three morphologies: basket, double-bouquet, and long-range GABAergic projection cells (Riedemann, 2019). Basket cells have axons that remain local and ramify extensively. Double-bouquet cells are mostly in supragranular layers and have translaminar axons collaterals that intertwine. Long-range GABAergic projection cells are expressed mainly in Layer VI and have axons that project to other brain areas (Riedemann, 2019).

The majority of SOM cells are MCs, and they comprise 15% of all cortical interneurons (Riedemann, 2019). They have egg-shaped soma and can have either a tufted or multipolar morphology. MCs have dense axonal ramifications locally, as well translaminar axon collaterals that ascend and arborize in Layer I (Hilscher et al., 2017). As MC axons ascend, collaterals innervate apical and basal dendrites of PCs in all layers. Layer-I arbors spread horizontally, to influence neighboring columns. Their axonal architecture enables MCs to modulate large numbers of PCs (Riedemann, 2019).

In mice, 50% of MCs are expressed in Layer II/III. There are a considerable number of MCs in Layer IV, and some expression in Layers V and VI (Riedemann, 2019, Hilscher et al., 2017). Possibly the most notable feature of MC cortical expression is that a portion of those expressed in Layer V also express α2nAChRs (Hilscher et al., 2017).

CHAPTER 1

Role of the α2nAChR subunit in A1 processing

of pure tone stimuli

Introduction

Optimization of nicotinic treatment for cognitive disorders, including auditory processing disorders necessitates a thorough understanding of how nAChR composition affects function, and how distribution and function integrate to affect cortical processing. While studies suggest the α2 subunit plays a critical role in learning and memory (Nakauchi et al., 2007; Jia et al., 2009; Kleeman et al., 2016; Lotfipour et al., 2017; Leão et al. 2012), its role in auditory processing is not known. Considering its sparse expression (<3% of cortical nAChR subunits) yet important function within the rodent hippocampus, and its high expression in primates (Hans et al., 2000), the understudied α2nAChR merits further investigation regarding possible important contributions to regulating cortical function and more specifically auditory processing. The focus of this study is the possible involvement of α2nAChRs in auditory processing, and whether it plays an integral role in the nicotinic enhancement of A1 responses to pure tone stimuli.

Materials and Methods

Animals

This study was conducted on postnatal day (PD) 60-75 α2KO (n = 16) mice, generated as described (Lotfipour et al., 2013), and WT (n = 17) littermates. In order to identify possible sex differences, both male (WT = 9; α2KO = 7) and female (WT = 8; α2KO = 9) mice were included in each group. Mice for all procedures were used in accordance with the National Institutes of Health *Guide for the Care and Use of Laboratory Animals* and as approved by the University of California, Irvine Institutional Animal Care and Use Committee (IACUC).

Surgeries

At PD60-75 male and female mice were anesthetized with urethane (0.7g/kg; Sigma) and xylazine (13mg/kg; Akorn), delivered via IP injection. Anesthesia was supplemented (IP injection) as needed, with additional urethane (0.14g/kg) and xylazine (1.3mg/kg). Urethane was chosen as the anesthesia for this study because it does not suppress nAChR function (Hara and Harris, 2002; Tassonyi et al., 2002).

Anesthetized, mice were placed in a sound-attenuating chamber (AC-3; IAC) and maintained at a body temperature of 37°C. Using a stereotaxic frame (model 923; Kopf Instruments) and blunt ear bars, the mouse's head was secured to a custom head holder with dental cement. A midline incision was made to access the skull, and a craniotomy was performed over the right temporal lobe region, exposing the brain for

25

CF mapping and electrode placement. Following the craniotomy, the brain was kept moist with saline warmed to 37°C. Ear bars were removed after confirming the skull was securely cemented to the custom head holder. Removing the ear bars allowed for presentation of pure tone stimuli.

Mapping for A1 and Determining Recording Site

Location and mapping of A1 for CF tonotopy was accomplished by presenting a standard set of pure tone stimuli (1–40 kHz in 2-kHz steps, 5 dB to 70 dB SPL in 5-dB steps) and using a glass micropipette filled with 1 M NaCl (~1 MΩ at 1 kHz), to record stimulus-evoked LFPs from multiple sites (~250 μm apart) along the anterior-posterior axis in Layer IV (400-μm depth). The frequency with the lowest threshold was identified for each recording site, to confirm the CF tonotopy expected for A1. This included a reversal of tonotopy where A1 borders with the anterior auditory field (Stiebler et al.,1997). Pure tone stimuli were digitally synthesized and controlled with MATLab (RP2.1 Enhanced Real-Time Processor) and emitted from a speaker (FF-1 with SA-1 Stereo Power Amp; Tucker-Davis Technologies) placed 3cm from mouse's left ear.

After mapping, the A1 site with the LFP of shortest onset latency (OL) and largest amplitude was selected as the site for multiprobe placement. A 16-channel multiprobe (2–3 MΩ at 1 kHz for each 177-μm^2 recording site, 100-μm separation between recording sites; NeuroNexus Technologies), was inserted in perpendicular orientation to the pial surface, at the selected site. Characteristic frequency (1-kHz steps) and

threshold (5-dB steps) were reidentified, based on LFPs recorded from 300–400 μm depth.
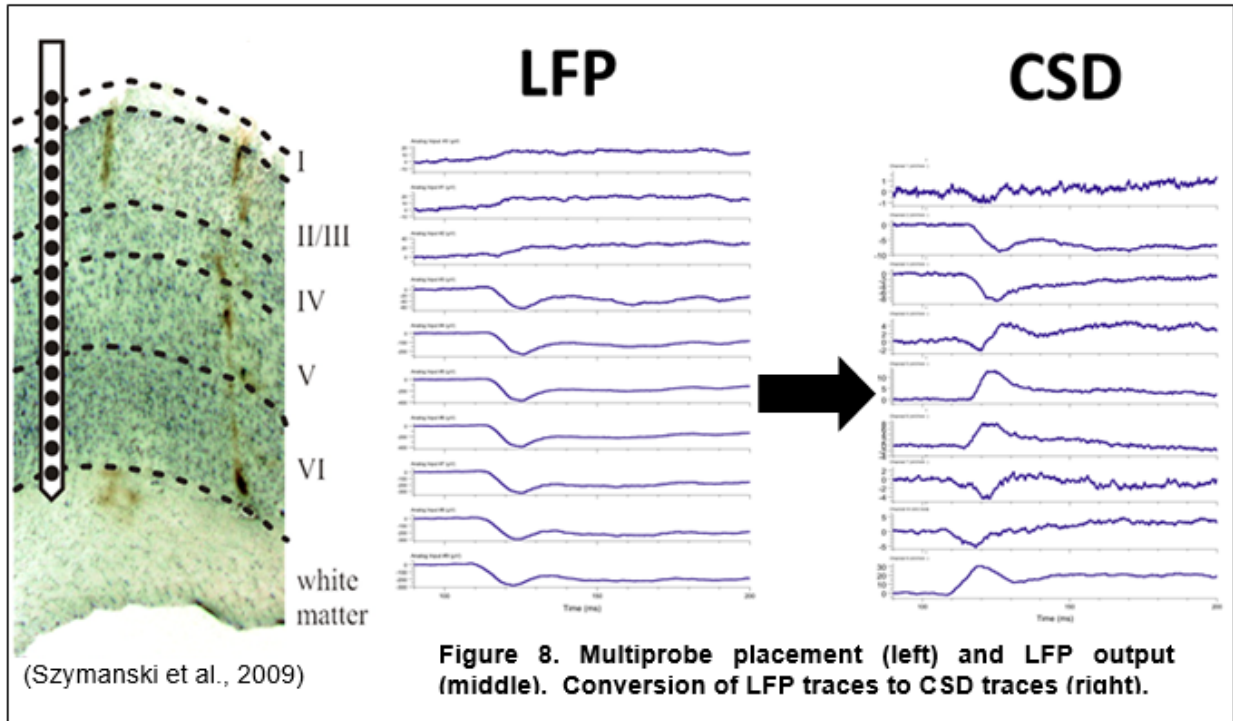
Electrophysiology Experiment and Acoustic Stimulation

Pure tone stimuli were digitally synthesized and controlled with MATLab (RP2.1 Enhanced Real-Time Processor) and emitted from a speaker (FF-1 with SA-1 Stereo Power Amp; Tucker-Davis Technologies) placed 3cm from mouse's left ear. Tones were 100ms in duration, with 5ms linear rise and fall ramps. During data collection, stimuli were delivered at a rate of 1/s in blocks of 25 trials.

With the multiprobe in place, pure tones were presented at CF (ranging 5-20 kHz across mice) and Th + 40dB. Each tone-evoked response used for analysis was the average LFP response to the block of 25 stimuli presentations (1/s). Subjects were exposed to stimuli blocks three times under each of three conditions: pre-saline, saline, and nicotine.

CSD profiles were converted from LFP profiles and analyzed (Figure 8). The middle-layer CSD trace with the shortest OL (typically 200 – 400 μm depth) marked the initial sink (referred to as 'Layer IV'). Response onset and initial slope were considered a reflection of monosynaptic thalamocortical input.

Using AxoGraph software, current sinks were measured in terms of OL, initial slope (over first 5ms), and amplitudes measured at 5ms and 20ms time points (after initial slope measurements). Time range for initial and time points for amplitude measurements were selected to distinguish between subcortical and intracortical influences on responses.

Figure 8. Multiprobe placement (left) and LFP output (middle). Conversion of LFP traces to CSD traces (right).

Nicotine Administration

Nicotine hydrogen tartrate salt (Sigma) was dissolved in saline (2.1 mg/kg free base), and delivered systemically, via subcutaneous injection. Because the effects of systemic nicotine on A1 tone-evoked responses last approximately 30 minutes (Kawai et al., 2011; Intskirveli and Metherate, 2012), pure tone presentations and recordings began within one minute after drug administration, and all post-nicotine data was collected within 20 minutes.

Data Analysis

AxoGraph software was used to analyze all response recordings. Statistical tests were carried out using GraphPad PRISM Version 9.1.2. All presented data are expressed as the mean ± standard error of the mean.

Each tone-evoked response used for analysis was the average response to 25 stimuli presentations, at regular intervals. As described in Kaur et al. (2005) and Kawai et al. (2007), CSD profiles were converted from LFP profiles (off-line) and analyzed.

One dimensional CSD profiles are the second spatial derivative of the LFP laminar profile (Muller-Preuss and Mitzdorf, 1984). Conventionally, a current sink reflects the location, timing, and magnitude of the underlying synaptic excitation. Layer IV was identified by the shortest-latency, middle-layer current sink (represents monosynaptic thalamorcortical and intracortical activity), which was used for analysis of OL, slope and amplitude. For CSD plots, response onset was defined as an amplitude exceeding three standard deviations from the baseline value, which was determined over the 100ms preceding the tone. Response onset was defined as the time-point (ms) at which the CSD trace met the response onset criterion. Response onset and initial slope reflected monosynaptic thalamocortical input from the medial geniculate body.

Slope and amplitude data for each subject were normalized to pre-saline condition. Onset latency data was not normalized. AxoGraph software was used to measure current sinks in terms of OL, slope (0-5ms time interval following response onset threshold), and amplitude (at 5ms and 20ms after onset threshold).

Group data was analyzed for possible sex differences using two-way repeated measures ANOVA (a = 0.05) for each mouse line. Because no sex differences were found, groups were collapsed across sex and data was analyzed using two-way mixed ANOVA (a = 0.05) for main effects (mouse line and conditions) and interactions, and Tukey's/Sidak's post-hoc tests for pairwise comparisons ("n" values represent number of mice).

In keeping with convention, the ANOVA for OL was conducted using absolute values (ms) for pre-saline, saline, and nicotine conditions. For all other parameters, values for saline and nicotine conditions were normalized to pre-saline responses before analyses.

Physiology Results

This study was conducted on adult (PD 60-75), C57 WT (M = 9; F = 8) and α2KO (M = 7; F = 9) mice. In order to identify possible sex differences, I included male and female subjects in both groups.

After mapping with a microelectrode to locate A1 in urethane-xylazine-anesthetized mice, I selected a recording site with robust responses to pure tone presentations at CF. I then inserted a 16-channel linear multiprobe with recording sites spaced 100 µm apart and spanning all six layers of the cortex. Pure tones were presented at that site's determined CF, 40dBs above determined threshold. Characteristic frequencies ranged from 5-20kHz across mice. Stimulus was presented in three blocks (25 presentations at regular intervals per block) under each of three conditions: pre-saline, post-saline, and nicotine.

The duration of acoustic stimulation under each condition was ~12 minutes, therefore acoustic stimulation under nicotine condition lasted less than the average half-life (~30min) for a single injection of nicotine (Intskirveli and Metherate, 2012). Tone-evoked responses used for analysis were the averaged (25 stimuli presentations) LFP responses within each block, converted (offline) into CSD profiles (Intskirveli and Metherate, 2012), as described in Kaur et al. (2005) and Kawai et al. (2007).

CSD traces at the shortest-latency, middle-layer current sinks were then analyzed using AxoGraph. Evoked responses were measured on parameters of OL, initial slope, and amplitude (as detailed in Methods section). Response onset criteria required an amplitude exceeding three standard deviations above baseline (the 100ms preceding stimuli). Slope was calculated from response onset to 5ms, and maximum amplitude at 5ms and 20ms after onset.

Using two-way ANOVAs, I checked for possible sex differences in each mouse line. No sex differences were found in either WT: OL ($F_{1, 15}$ =0.394, p = 0.540); Slope (Slope: $F_{1, 15}$ = 1.154, p = 0.300); 5ms Amp ($F_{1, 15}$ = 0.287, p = 0.600); or 20ms Amp (Amp: $F_{1, 15}$ = 0.427, p = 0.523); or KO: OL ($F_{1, 14}$ =2.584, p = 0.104;); Slope (Slope: $F_{1, 14}$ = 0.388, p = 0.543); 5ms Amp ($F_{1, 14}$ = 1.039, p = 0.325), or 20ms Amp (Amp: $F_{1, 14}$ = 0.012, p = 0.915) mouse lines (graphs not included). Therefore, data for each group were collapsed across sex for all subsequent analyses.

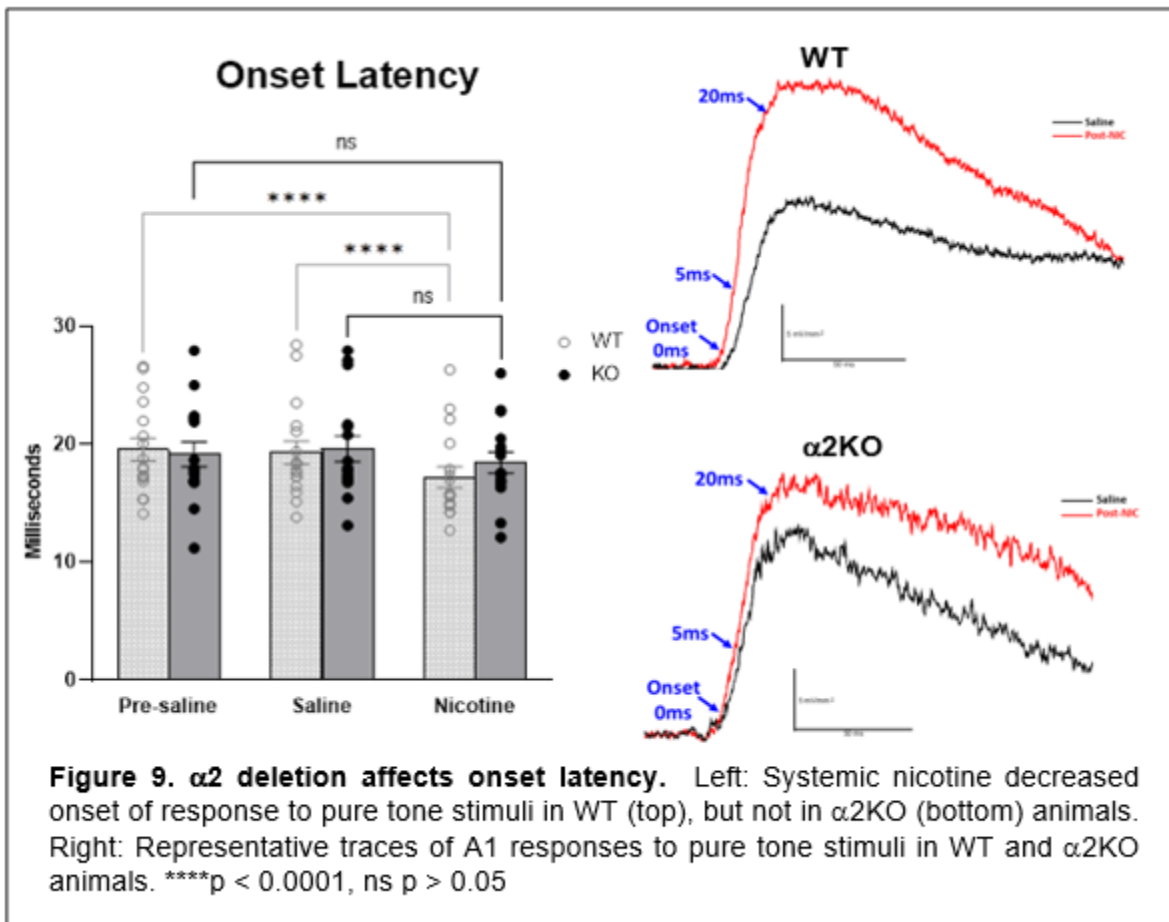Using two-way ANOVAs, I examined possible effects of mouse line (WT vs. α2KO) and drug condition on A1 responses to pure tones. Each subject was exposed to three conditions (pre-saline, saline, and nicotine) of the drug factor. There were main

effects of Conditions on all parameters (n = 33; OL: $F_{2, 62}$ = 19.32, p < 0.0001; Slope: $F_{2, 62}$ = 36.55, p < 0.0001; 5ms Amp: $F_{1, 31}$ = 47.83, p < 0.0001; 20ms Amp: $F_{1, 31}$ = 48.96, p < 0.0001) (Figures 9-11).
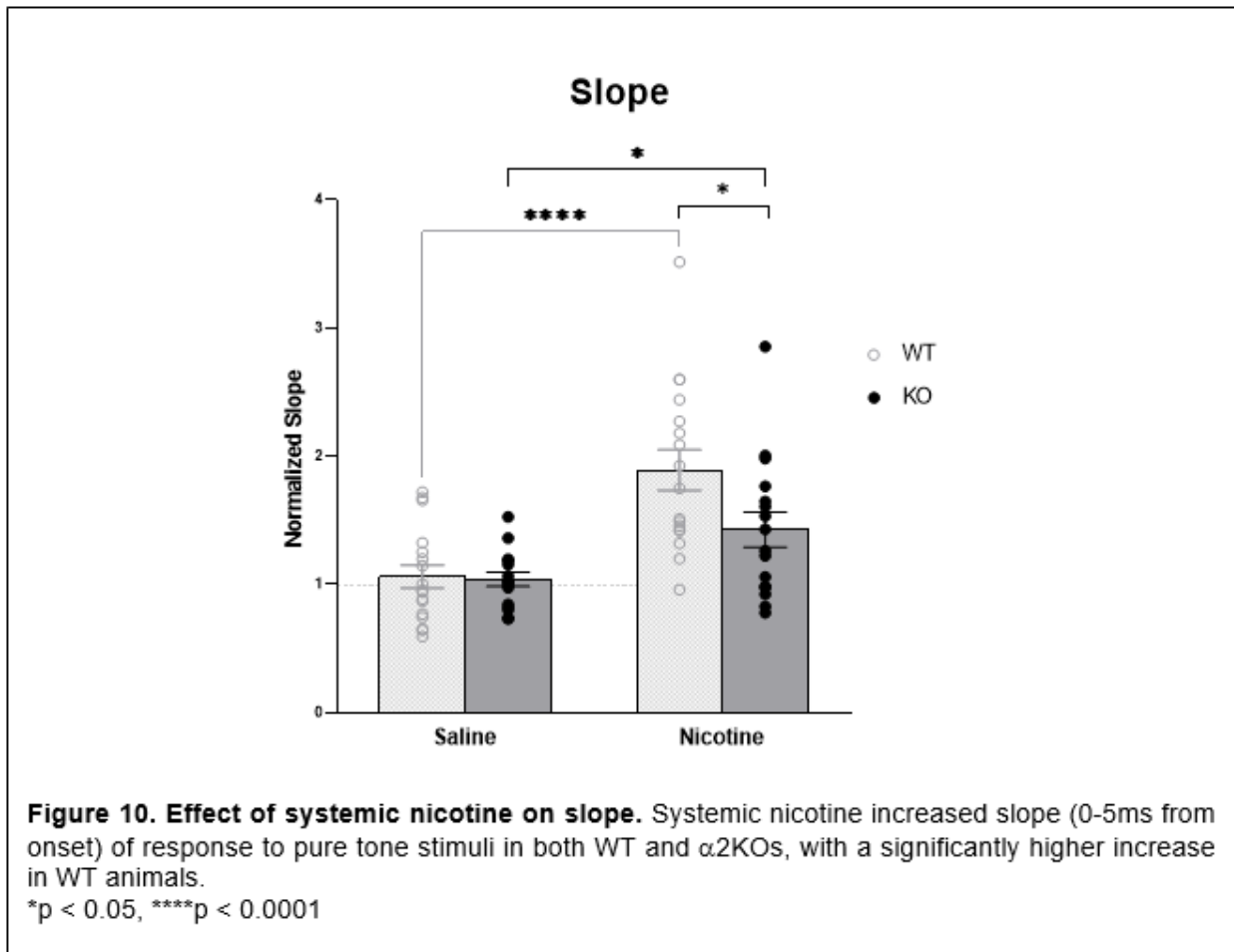
Onset latency

For **OL**, there was a main effect of mouse line ($F_{1, 31}$ = 8.410, p = 0.007), and an interaction of condition x mouse line ($F_{2, 62}$ = 4.709, p = 0.0125), where nicotine reduced the OL for responses in WT but not α2KO animals (t_{31} = 3.941, p = 0.001) (Figure 9). Onset latency for α2KO group showed no significant difference between pre-saline, saline, and nicotine conditions.

Figure 9. α2 deletion affects onset latency. Left: Systemic nicotine decreased onset of response to pure tone stimuli in WT (top), but not in α2KO (bottom) animals. Right: Representative traces of A1 responses to pure tone stimuli in WT and α2KO animals. ****p < 0.0001, ns p > 0.05
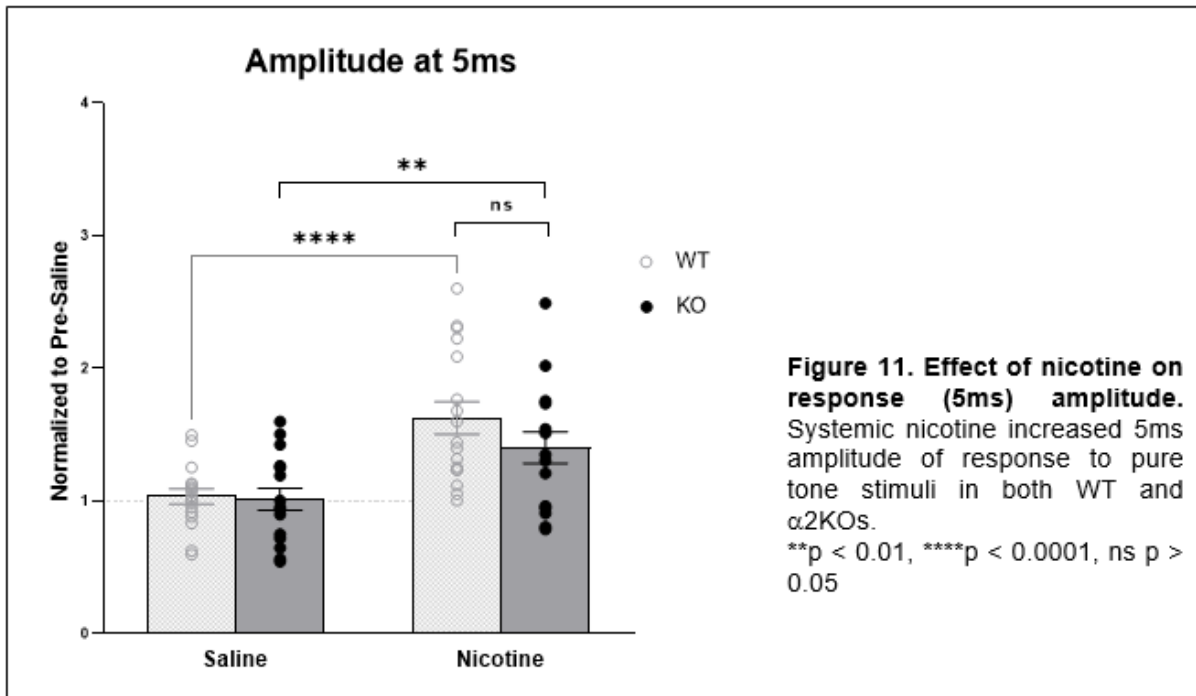
Slope

For **slope**, there was no main effect of mouse line ($F_{1, 31}$ = 2.977, p = 0.094). Both WT (t_{32} = 6.562, p < 0.0001) and α2KO (t_{32} = 2.979, p = 0.011) showed a significant increase in slope after administration of nicotine (Figure 10). However, there was an interaction of conditions x mouse lines ($F_{1, 31}$ = 5.911, p = 0.021) in that, slope increase for WT was significantly greater than for α2Os (t_{32} = 2.771, p = 0.015).

Figure 10. Effect of systemic nicotine on slope. Systemic nicotine increased slope (0-5ms from onset) of response to pure tone stimuli in both WT and α2KOs, with a significantly higher increase in WT animals.
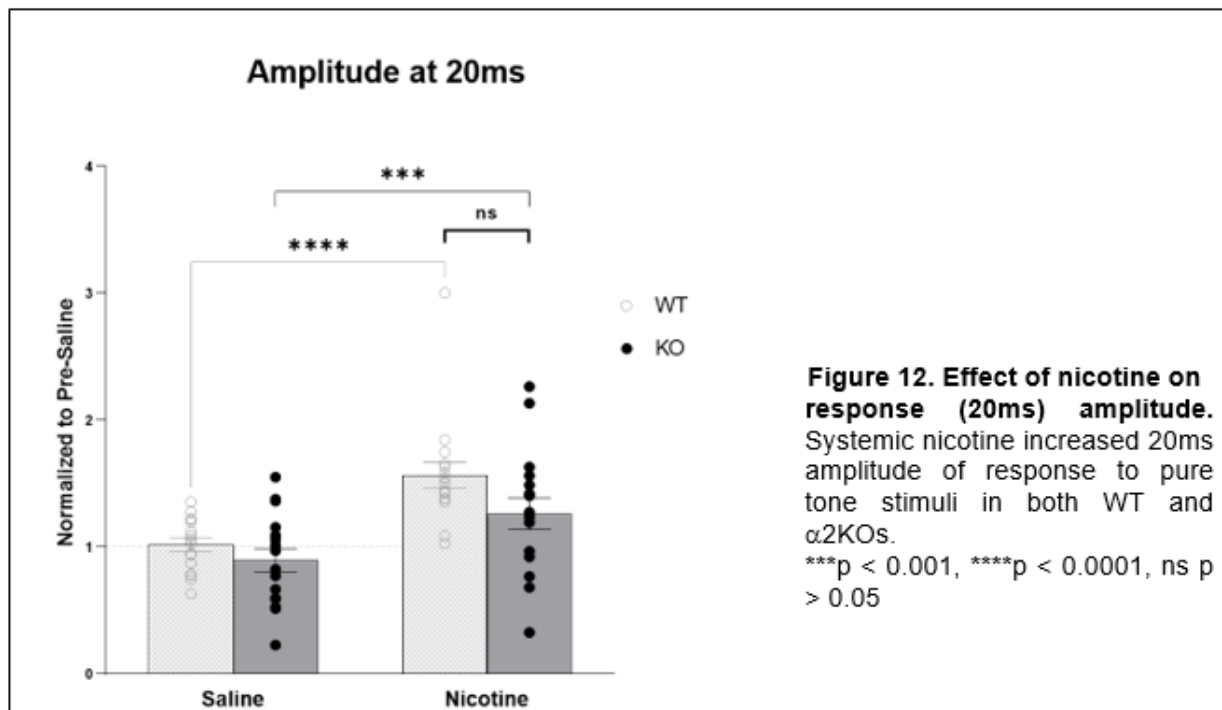*p < 0.05, ****p < 0.0001

Amplitude: 5ms and 20ms

For 5ms and 20ms Amplitude measurements, there was no main effect of mouse line (5ms Amp: $F_{1, 31}$ = 1.036, p = 0.317; 20ms Amp: $F_{1, 31}$ = 3.201, p = 0.0834). There was no

interaction of conditions x mouse line for either 5ms ($F_{1, 31}$ = 2.074, p = 0.1599) or 20ms

($F_{1, 31}$ = 1.839, p = 0.1848) amplitude measurements (Figures 11 and 12). Nicotine

increased 5ms Amplitude in both WT (t_{33} = 6.000, p < 0.0001) and α2KO (t_{31} = 3.815, p =

0.001) animals. Nicotine also caused an increase in 20ms Amplitude in both WT (t_{33} =

5.998, p < 0.0001) and α2KO (t_{32} = 3.929, p = 0.0009) animals. Thus, deletion of

α2nAChR subunit resulted in the loss of nicotine's effect on onset and initial

Slope, but nicotine still enhanced response amplitude at 5ms and 20ms.

Figure 11. Effect of nicotine on response (5ms) amplitude. Systemic nicotine increased 5ms amplitude of response to pure tone stimuli in both WT and α2KOs.
**p < 0.01, ****p < 0.0001, ns p > 0.05

Amplitude at 20ms

Figure 12. Effect of nicotine on response (20ms) amplitude. Systemic nicotine increased 20ms amplitude of response to pure tone stimuli in both WT and α2KOs.
***$p < 0.001$, ****$p < 0.0001$, ns $p > 0.05$

Discussion

This loss of function study investigated the role of α2nAChRs in the processing of pure tone stimuli. I administered nicotine systemically to WT and α2KO mice, presented pure tone stimuli, then compared A1 responses on the basis of OL, initial slope, and 5ms/20ms amplitude (Figures 9-12).

In WT animals, nicotine decreased response onset latency and increased both response slope and amplitude. However, deletion of the α2nAChR subunit altered nicotine's effects for both response onset and initial slope. Specifically, time to onset did not decrease with nicotine on board. Additionally, although slope increased after nicotine administration, the increase was significantly smaller compared to that of WT animals. Deletion of the α2nAChR subunit did not change nicotine's effects on 5ms and 20ms amplitudes, as there were increases in response amplitudes for both WT and α2KOs, without a significant difference between groups. These results suggests that the nicotinic enhancement of initial response measures (onset/initial slope) and later measures (5ms, 20ms amplitudes) are mediated differentially.

To interpret these results, it is useful to consider the effects of both thalamocortical (TC) input and intracortical activity on A1 responses to stimuli. The following explanation/example, though simplified, is gleaned from Metherate et al., (2015) and Intskirveli et al., (2016). Tone presentations at CF elicit direct corresponding TC input to A1 neurons in Layer IV (input layer). As such, the OL and initial slope of A1 responses reflect subcortical, monosynaptic (TC) input. Afterward, cortical neurons instantaneously relay input information locally and across ACx. Within milliseconds of

TC input, the original monosynaptic signal has been conveyed (via intracortical APs) to "second-set" cortical neurons. These cortical neurons are activated by intracortical (polysynaptic) signaling. This activation takes time, and recorded responses of second-set neurons are reflected several milliseconds after the original neuronal response. Therefore, traces of A1 responses reflect TC input at OL (0ms) and during the first few milliseconds afterward (i.e., initial slope). The farther (temporally) traces get from response onset, the more they reflect intracortical activity. In this study, OL for α2KOs remained unaltered with nicotine, and slope, although greater than the saline condition, was still significantly lower than in WT animals. These results suggest that α2nAChR-mediated effects of nicotine originate in receptors located subcortically.

CHAPTER 2

Colocalization of α2-subunit with interneurons containing VIP, PV, or SOM in mouse auditory cortex

Introduction

Chapter 1 experiments compared the nicotinic enhancement of A1 responses to pure tone stimuli across WT and α2KO mouse lines. Results indicated physiological differences, suggesting that α2nAChRs help mediate the enhancement seen in WT mice. Because anatomy often helps explain physiology, I investigated the distribution of α2 subunit expression within ACx, including possible sex differences.

Hilscher et al., (2017) uncovered that 29.1% of α2 subunit-expressing cells in Layer V of A1 cortex also expressed SOM. Of that population, 37 biocytin-filled cells were tested and 97.3% could be identified as deep-layer MCs. However, cell type(s) for the remaining fraction (70.9%) of α2 subunit-containing cells in LV were not identified. Here, we used α2eGFP in conjunction with immunolabeling of PV, VIP, and SOM cells, to verify the laminar distribution of α2nAChRs in the ACx and characterize α2-subunit colocalization with these three (largest) classes of GABAergic interneurons. Immunolabeling of the α2 subunit protein was not possible, as antibodies to recognize it have yet to be developed.

Materials and Methods

Animals

This study was conducted on Chrna2-eGFP BAC (Tg(Chrna2-EGFP)OF8Gsat/Mmucd) transgenic mice. Frozen sperm was obtained from Mutant Mouse Resource & Research Center, UC Davis, and mice were reanimated in UCI's Transgenic Mouse Facility. Mice for all procedures were used in accordance with the National Institutes of Health *Guide for the Care and Use of Laboratory Animals* and as approved by the University of California, Irvine Institutional Animal Care and Use Committee (IACUC).

Sectioning and Staining

At PD60, male and female α2 eGFP mice were deeply anesthetized (urethane 0.7g/kg ip; Xylazine 13mg/kg ip) and perfused in a transcardial manner, with ice-cold phosphate-buffered saline (PBS, 0.1 M sodium phosphate, 0.9% NaCl), followed by 4% paraformaldehyde (PFA) ~10ml/min for 10 minutes. Brains were harvested and fixed overnight (4% PFA; 4°C). Afterward, brains were rinsed in PBS and sectioned (40- μm) along the thalamocortical plane (Cruikshank et al., 2001), using a Leica VT1000P vibratome. Sections were rinsed three (3) times in PBS and incubated for 90 minutes in a blocking solution of 5% donkey serum (Sigma) and 0.3% Triton X-100 (TX-100, Sigma) in PBS at room temperature.

PV staining - after blocking, sections were incubated overnight (4°C), in a solution containing mouse monoclonal, anti-parvalbumin antibody (1:1000 Dilution, Millipure

39

Sigma) and blocking solution of 5% donkey serum and 0.3% Triton X-100 in PBS at room temperature. The following day, sections were washed and incubated in Alexa fluor 488 donkey anti-mouse IgG (H+L) (1:1000 Dilution, Invitrogen) for two hours at 20°C.

VIP staining - after blocking, sections were incubated overnight (4° C), in a solution containing mouse monoclonal, anti-VIP IgG$_{2b}$ antibody (1:500 Dilution, Santa Cruz biotechnology) and blocking solution of 5% donkey serum and 0.3% Triton X-100 in PBS at room temperature. The following day, sections were washed and incubated in Alexa fluor 488 donkey anti-mouse IgG (H+L) (1:1000 Dilution, Invitrogen) for two hours at 20° C.

SOM staining - after blocking, sections were incubated overnight (4° C), in a solution containing rat monoclonal, anti-SOM clone YC7 antibody (1:500 Dilution, Millipure Sigma) and blocking solution of 5% donkey serum and 0.3% Triton X-100 in PBS at room temperature. The following day, sections were washed and incubated in Alexa fluor 488 donkey anti-rat IgG (H+L) (1:250 Dilution, Invitrogen) for two hours at 20°C.
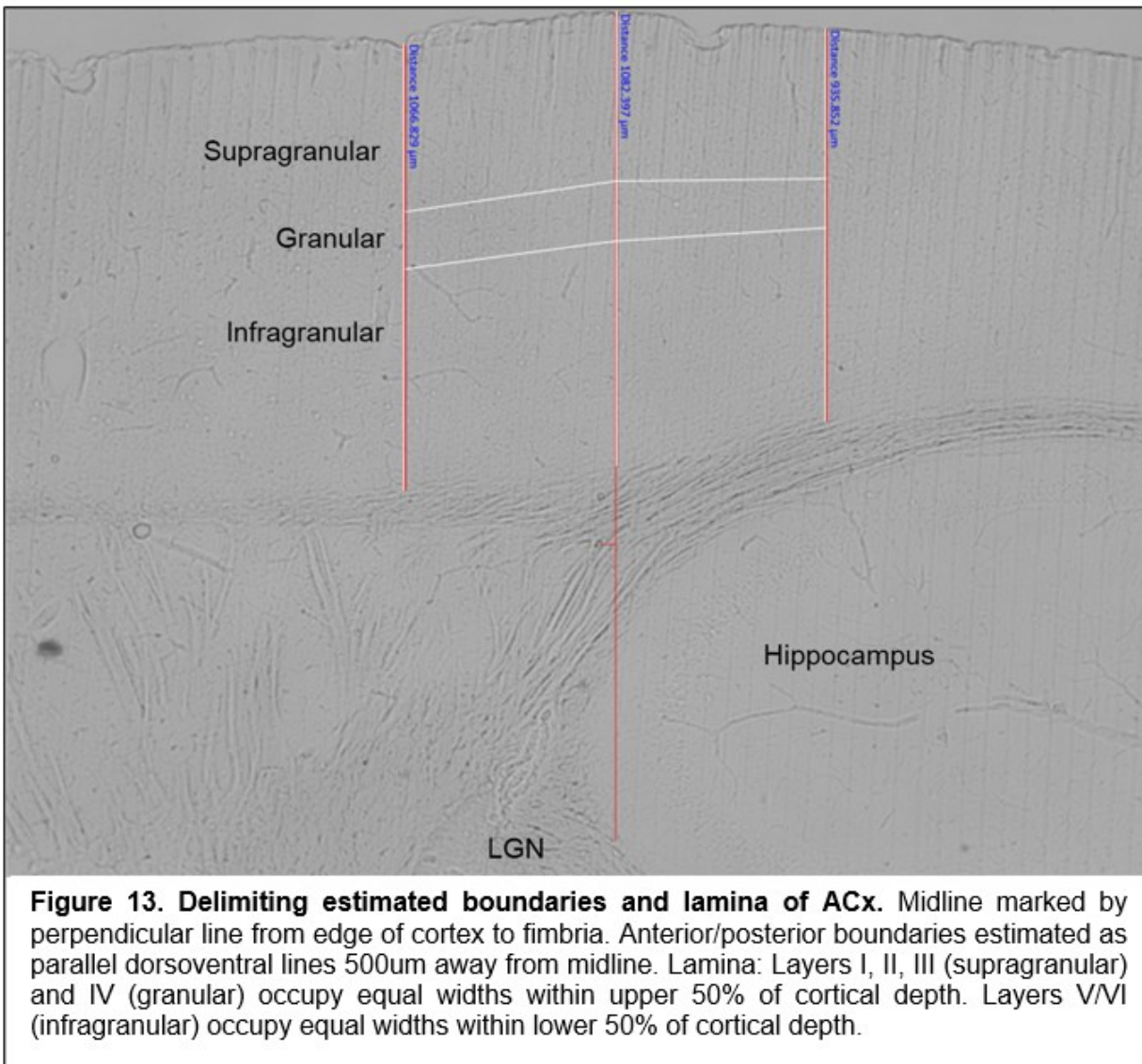
Stained sections were washed three (3) times for 10 minutes in PBS and mounted onto glass slides with Glycergel mounting medium (Dako), for analysis.

Cell Counting

A Zeiss Axioskop microscope equipped with a Zeiss Axiocam digital camera and a fluorescent light source (X-Cite; 120 Q Series, EXFO Photonic Solution) was used for this study. Zen imaging software (Zeiss) was used to image, process and store images in

fluorescence and normal light and at different magnifications.

To estimate the boundaries of the auditory cortex in thalamocortical sections, I first constructed a line beginning at the base of the fimbria (where it meets the hippocampus) and ending in a 90° angle at the edge of the cortex (Figure 13). This

Figure 13. Delimiting estimated boundaries and lamina of ACx. Midline marked by perpendicular line from edge of cortex to fimbria. Anterior/posterior boundaries estimated as parallel dorsoventral lines 500um away from midline. Lamina: Layers I, II, III (supragranular) and IV (granular) occupy equal widths within upper 50% of cortical depth. Layers V/VI (infragranular) occupy equal widths within lower 50% of cortical depth.

marked the midline of the auditory cortex. I then constructed a perpendicular line (500um) on either side of the midline. By drawing perpendicular lines (parallel to midline) at the ends of the 500um lines, I marked the anterior and posterior borders of

41

the analysis region within auditory cortex. To identify cortical thickness, I adjusted (visually) the length of the three parallel lines so that they spanned between the ventral and dorsal edges of the cortex. Together, these marked the boundaries of the area I analyzed. To delimit Layers I-III, IV, and V/VI I used the following laminar proportions (Anderson et al. 2009): Layers I-IV occupied equal widths within the upper 50% of the cortex, and Layers V/VI occupied equal widths within the lower 50%.

After estimating the location of ACx, I determined the laminar distribution and average cell counts of PV, VIP, and SOM immunolabeled cells, as well as their respective colocalization with eGFP tagged cells containing α2 nAChR subunits.

Data Analysis

Considering possible sex differences, data was analyzed using two-way ANOVAs (a = 0.05) for main effects (layer/sex) and interactions. Because no sex differences were found, groups were collapsed, and data was analyzed using one-way ANOVAs (a = 0.05) and Tukey's post-hoc tests for pairwise comparisons.

IHC Results

This study was conducted on adult (PD 60-65), transgenic α2eGFP expressing mice (see Methods). In order to investigate possible sex differences, I included both male (n = 6) and female (n = 4) subjects.
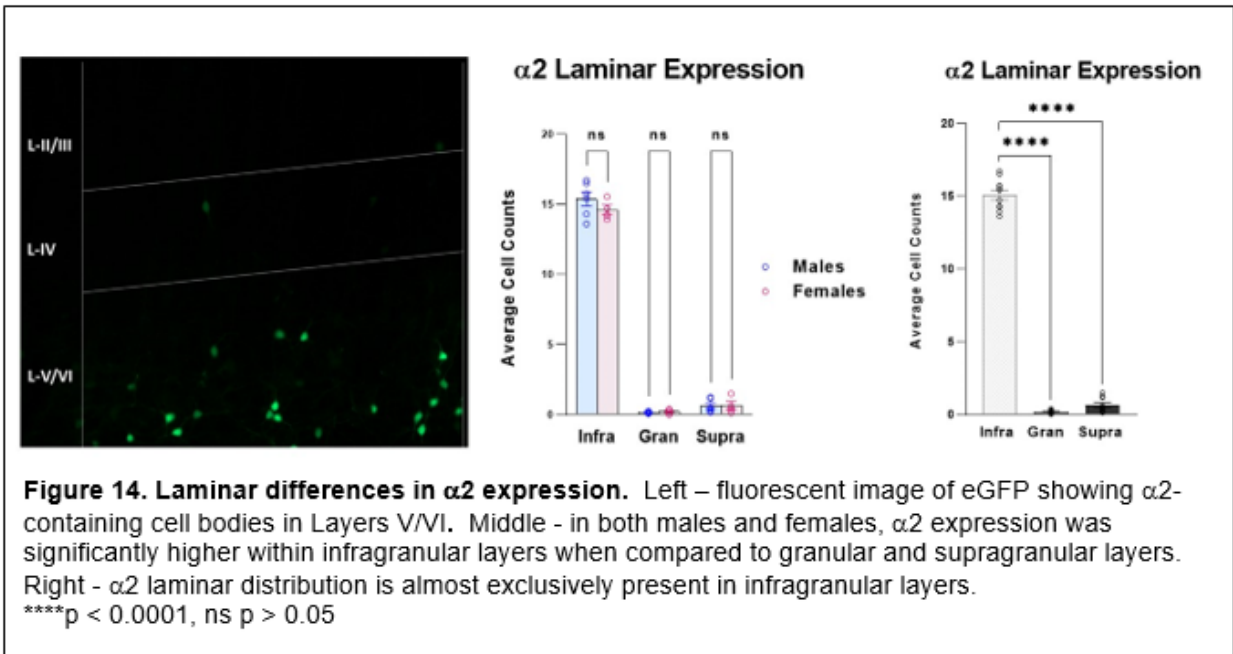
After brains were harvested, sectioned, and immunohistochemically stained for PV, VIP, or SOM expression, sections were imaged using Zeiss Axiocam digital camera and Zen imaging software. Boundaries for ACx and infragranular, granular and

supragranular layers were determined, and distribution of α2 nAChR subunits and their colocalization with VIP, PV, and SOM immunolabeled cells was calculated.

I measured PV, VIP, SOM and α2 eGFP expression in supragranular, granular and infragranular layers, as well as colocalization of α2 eGFP with respective immunolabeled cells. Using two-way ANOVAs, I checked for differences in laminar expression, colocalization and differences across sex.
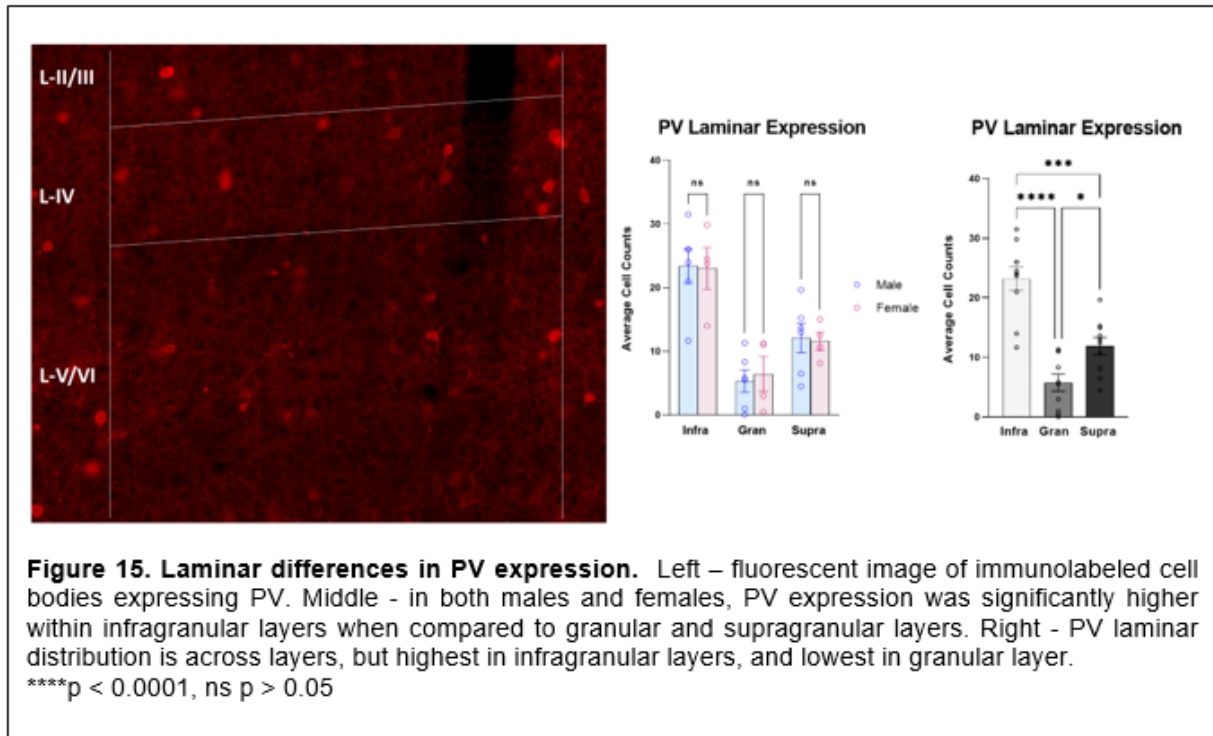
α2nAChR subunit laminar expression

α2 laminar expression concentrated in the infragranular layers, as there was minimal expression elsewhere. Two-way ANOVA results (Figure #) showed a main effect of Layer ($F_{2, 24}$ = 1453, p < 0.0001) for Sex ($F_{1, 24}$ = 0.810, p = 0.380), and no Layer x Sex interaction effect ($F_{2, 24}$ = 1.109, p = 0.346). Post hoc comparisons (Figure 14) of differences across layers showed α2 expression within infragranular layers was

Figure 14. Laminar differences in α2 expression. Left – fluorescent image of eGFP showing α2-containing cell bodies in Layers V/VI. Middle - in both males and females, α2 expression was significantly higher within infragranular layers when compared to granular and supragranular layers. Right - α2 laminar distribution is almost exclusively present in infragranular layers.
****p < 0.0001, ns p > 0.05

significantly higher than in the granular (t_{18} = 68.74, p < 0.0001) and supragranular (t_{18} = 66.65, p < 0.0001) layers. There was no significant difference in expression between supragranular and granular (t_{18} = 2.095 p = 0.315).

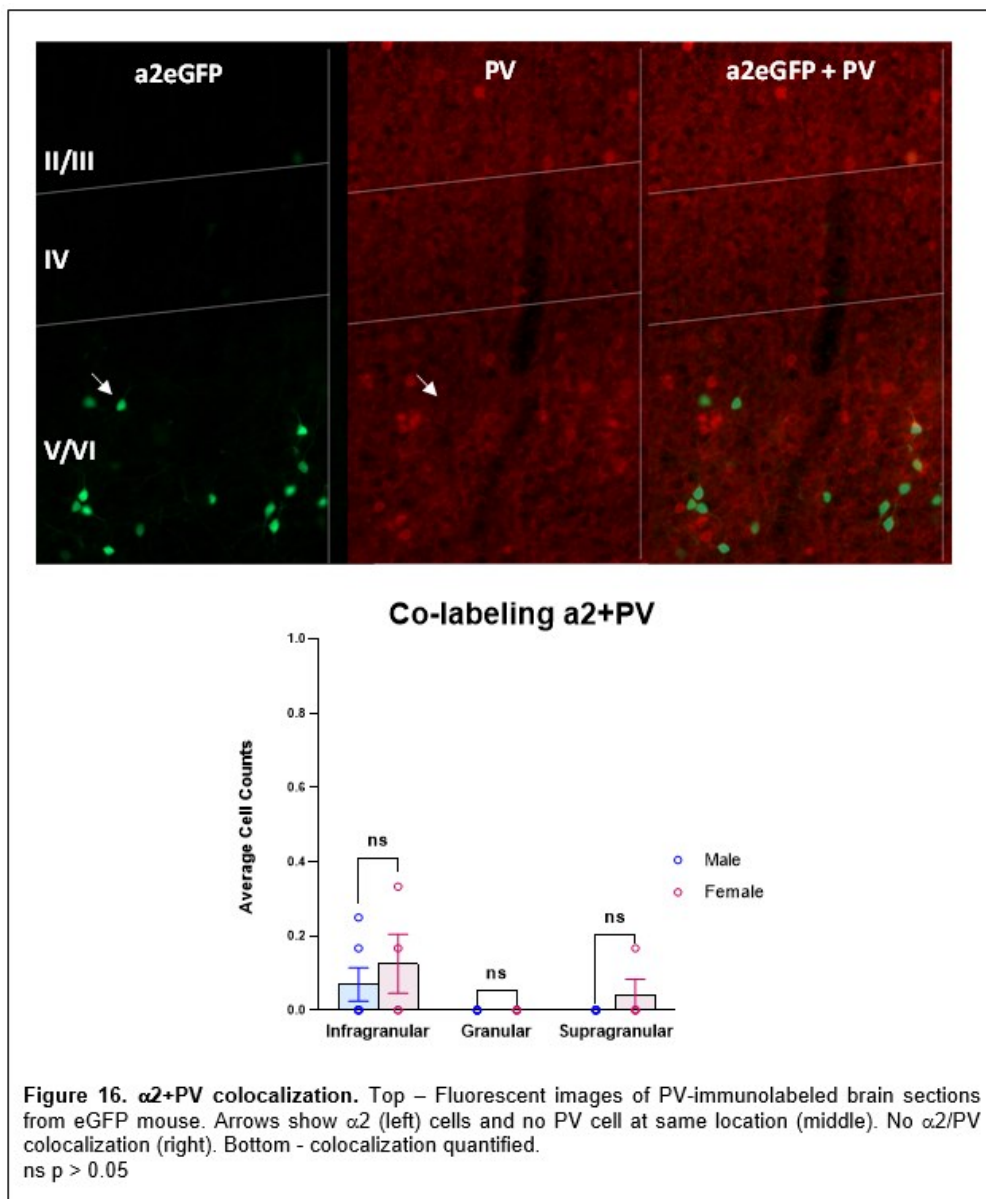*PV laminar expression and colocalization with α2*

PV expression was in line with existing literature, in that PV cells were expressed in all layers except Layer I, but mostly in infragranular layers. Granular layers showed the least PV expression (Figure 15).

Figure 15. Laminar differences in PV expression. Left – fluorescent image of immunolabeled cell bodies expressing PV. Middle - in both males and females, PV expression was significantly higher within infragranular layers when compared to granular and supragranular layers. Right - PV laminar distribution is across layers, but highest in infragranular layers, and lowest in granular layer. ****p < 0.0001, ns p > 0.05

Two-way ANOVA results showed a main effect of Layer ($F_{2, 24}$ = 24.68, p < 0.0001). There was no main effect of Sex ($F_{1, 24}$ = 0.002, p = 0.968), and no Layer x Sex interaction effect ($F_{2, 24}$ = 0.063, p = 0.939). Post hoc comparisons (Tukey's) showed that overall PV expression was significantly higher in infragranular layers when compared to
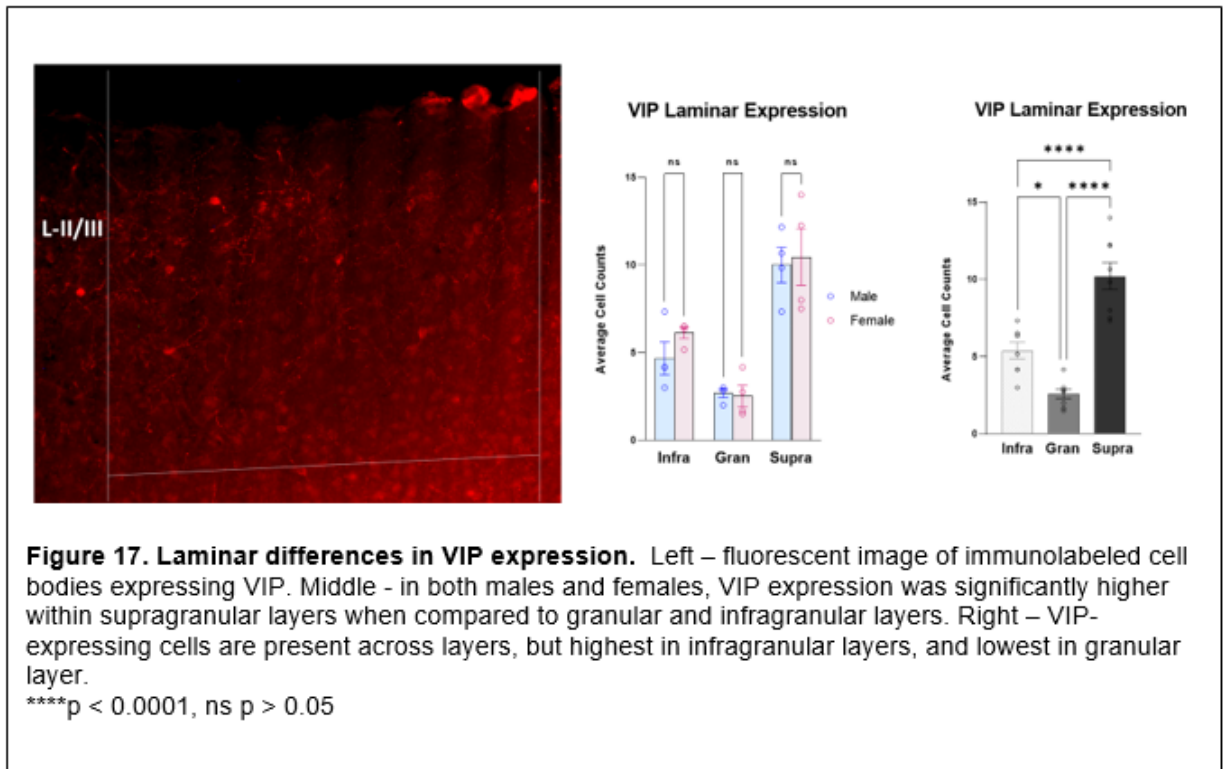
granular (t_{18} = 10.65, $p < 0.0001$) and supragranular (t_{18} = 6.91, $p = 0.0001$) layers. PV

expression in granular layer was significantly higher than in supragranular layers (t_{18} =

3.73, $p = 0.035$).

Overall, PV showed negligible colocalization with the $\alpha2$ protein (Figure 16). The

two-way ANOVA indicated a main effect of Layer ($F_{2, 24}$ = 3.807, $p = .037$). However,

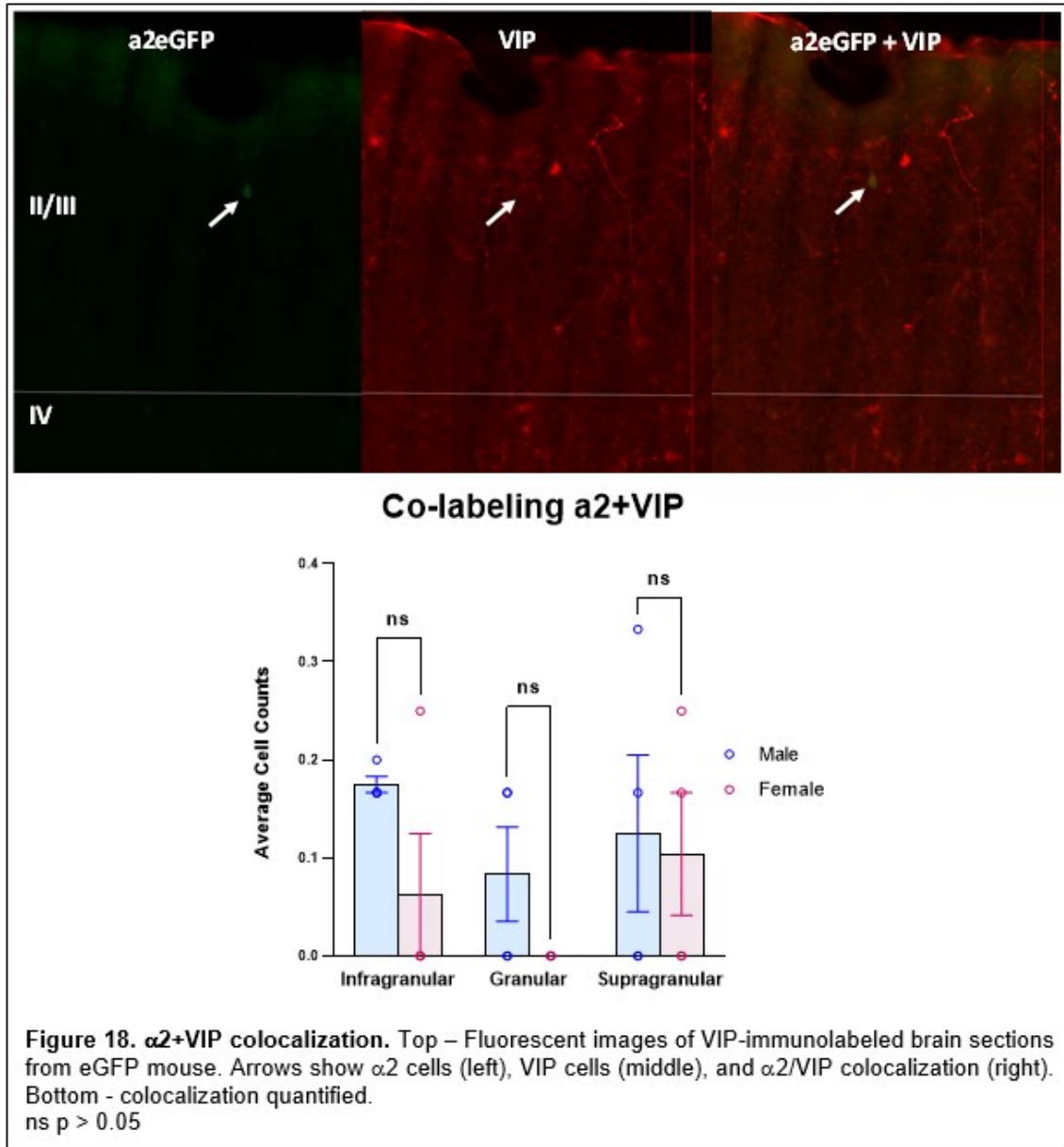post hoc comparisons (Tukey's) did not find a significant difference between in any

Figure 16. $\alpha2$+PV colocalization. Top – Fluorescent images of PV-immunolabeled brain sections from eGFP mouse. Arrows show $\alpha2$ (left) cells and no PV cell at same location (middle). No $\alpha2$/PV colocalization (right). Bottom - colocalization quantified.
ns $p > 0.05$

comparison. There was no main effect of Sex ($F_{1, 24}$ = 1.145, p = 0.295), and no Layer x

Sex interaction effect ($F_{2, 24}$) = 0.304, p = 0.741).

VIP laminar expression and colocalization with $\alpha2$ The highest expression of VIP cells

was in supragranular layers (Figure 17). This finding also supports existing literature.

Two-way ANOVA showed a main effect of Layer ($F_{2, 18}$ = 35.94, p < 0.0001). There was

no main effect of Sex ($F_{1, 18}$ = 0.617, p = 0.443), and no Layer x Sex interaction effect ($F_{2, 18}$ = 0.398, p = 0.677). Post hoc comparisons (Tukey's) showed significant

Figure 17. Laminar differences in VIP expression. Left – fluorescent image of immunolabeled cell bodies expressing VIP. Middle - in both males and females, VIP expression was significantly higher within supragranular layers when compared to granular and infragranular layers. Right – VIP-expressing cells are present across layers, but highest in infragranular layers, and lowest in granular layer.
****p < 0.0001, ns p > 0.05

differences in VIP expression when comparing infragranular and granular layers (t_{14} = 4.53, p = 0.011); infragranular and supragranular layers (t_{14} = 7.80, p < 0.0001); and granular and supragranular layers (t_{14} = 12.33, p < 0.0001). There was virtually no VIP/$\alpha2$ colocalization in any layer (Figure 18). Two-way ANOVA showed no main effects
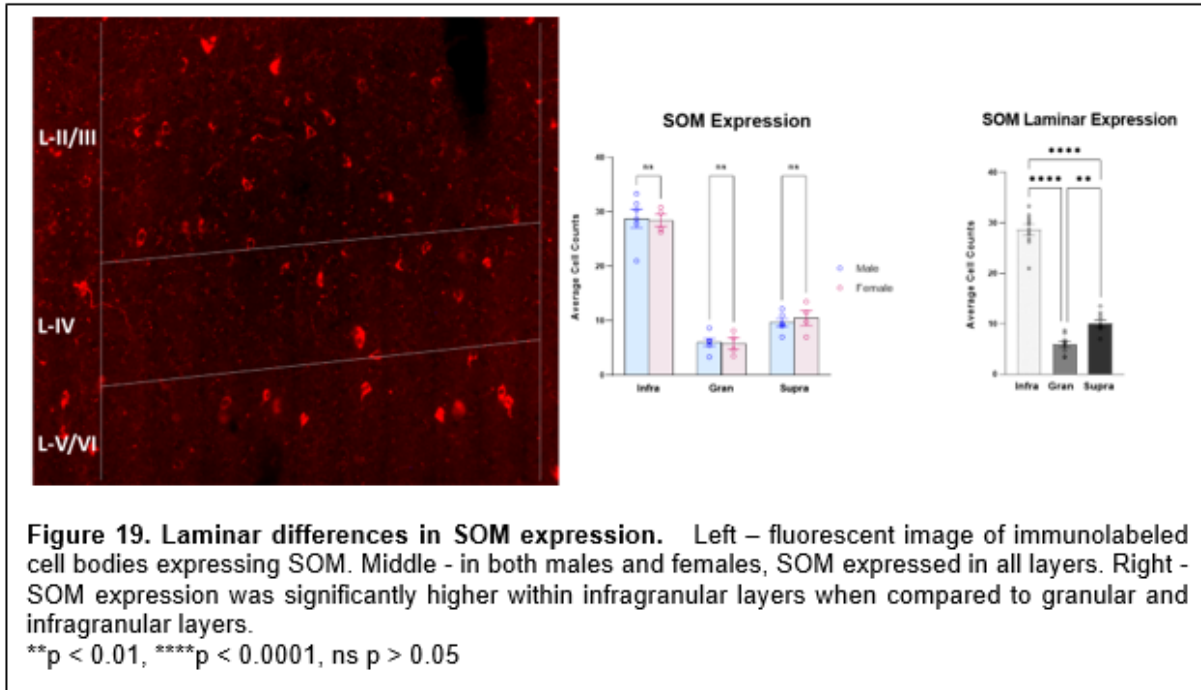
of Layer ($F_{2, 18}$ = 1.362, p = 0.281) or Sex ($F_{1, 18}$ = 2.834, p = 0.110), and no interaction of Layer x Sex (F2, 18 = 0.397, p = 0.678).

Figure 18. α2+VIP colocalization. Top – Fluorescent images of VIP-immunolabeled brain sections from eGFP mouse. Arrows show α2 cells (left), VIP cells (middle), and α2/VIP colocalization (right). Bottom - colocalization quantified.
ns p > 0.05

SOM laminar expression and colocalization with α2

SOM cells expressed mostly in infragranular layer, with moderate to minimal expression resulted in other laminae (Figure 19).   A two-way ANOVA for SOM

expression resulted in a main effect of Layer ($F_{2, 24}$ = 193.9, p < 0.0001). There was no main effect of Sex ($F_{1, 24}$ = 0.004, p = 0.951), and no Layer x Sex interaction ($F_{2, 24}$ = 0.133, p = 0.876). Tukey's post hoc comparisons showed that infragranular layers had

Figure 19. Laminar differences in SOM expression. Left – fluorescent image of immunolabeled cell bodies expressing SOM. Middle - in both males and females, SOM expressed in all layers. Right - SOM expression was significantly higher within infragranular layers when compared to granular and infragranular layers.
**p < 0.01, ****p < 0.0001, ns p > 0.05

significantly more SOM expression than both granular (t_{18} = 28.16, p < 0.0001), and supragranular (t_{18} = 23.15, p < 0.0001) layers. There was also a significant difference in expression between granular and supragranular layers (t_{18} = 5.005, p < 0.004).

SOM/α2 colocalization was greater than with PV or VIP cells (Figure 20). In fact, colocalization was almost exclusively with cells expressing SOM. There was a main effect of Layer ($F_{2, 24}$ = 54.22, p < 0.0001). There was no main effect of Sex ($F_{1, 24}$ = 0.817, p = 0.375), and no Layer x Sex interaction ($F_{2, 24}$ = 0.675, p = 0.519). Tukey's post hoc comparisons indicated higher SOM/α2 colocalization within infragranular layers

when compared to granular (t_{18} = 13.54, p < 0.0001) and supragranular (t_{18} = 13.48, p < 0.0001) layers (Figure 20). There was no significant difference in colocalization between granular and supragranular layers (t_{18} = 0.056, p > 0.999).

Figure 20. α2+SOM colocalization.
In both males and females α2 colocalization with SOM was significantly higher within infragranular layers when compared to granular and infragranular layers (in which colocalization was negligible). ***p < 0.001, ****p < 0.0001
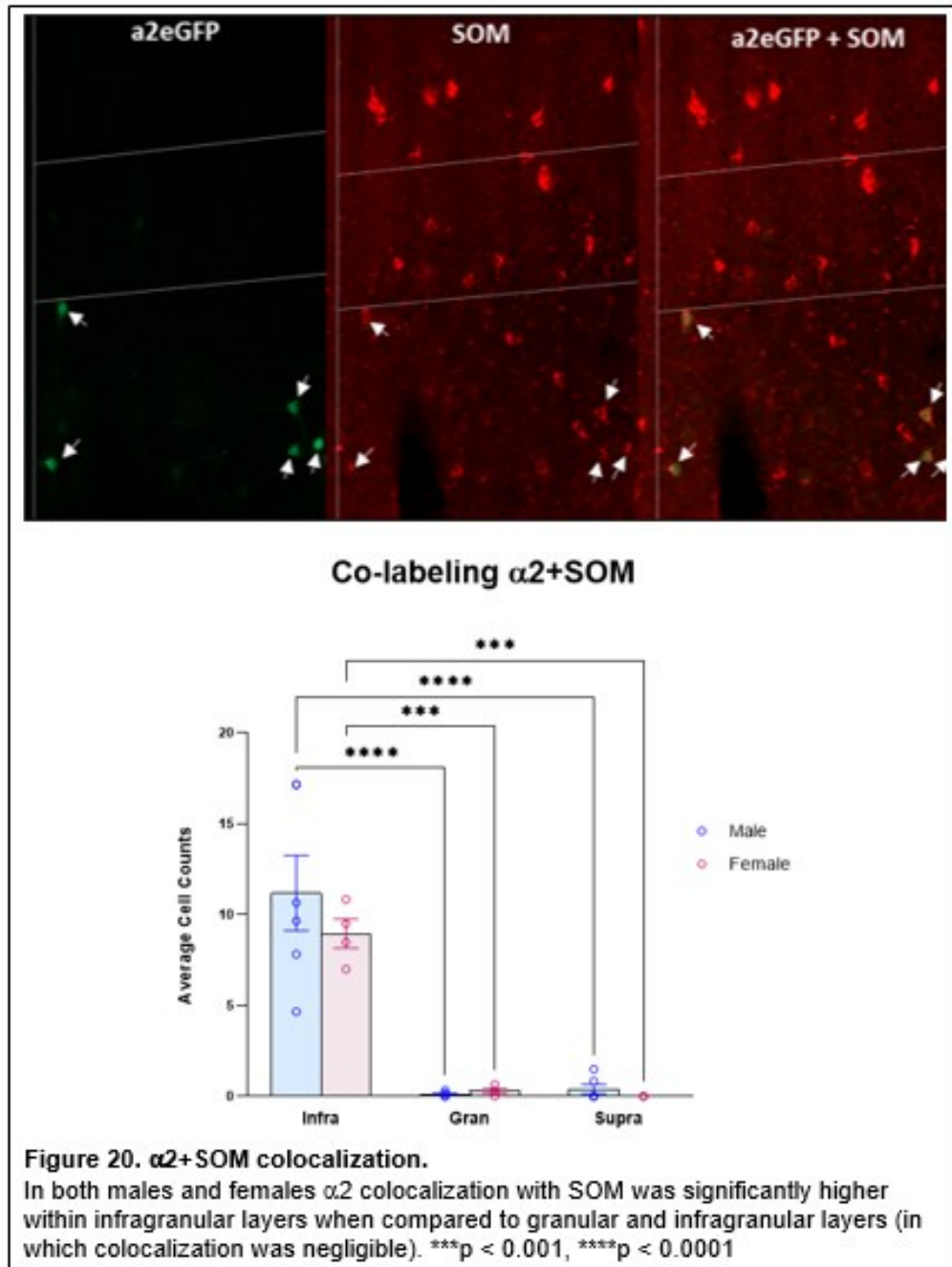
Discussion

The focus of this project was to expand what is currently known about α2nAChR expression within ACx. To this end, after brain tissue was sectioned stained and imaged, I measured the laminar expression of α2nAChR subunit, PV, VIP, and SOM in male and female mice, as well as the colocalization of α2nAChR with the above three interneuron markers.

PV cells are found in all layers except Layer I (Rudy et al., 2011). We found PV expression in supragranular, granular and infragranular layers, but predominantly in infragranular layers and least in the granular layer. Expression was significantly different in all groups. VIP cells are most dense in Layer II/III (Rudy et al., 2011). Our results are in line with that observation, as we found expression in all layers except Layer I, with the highest expression of VIP in the supra granular layers, and the lowest in granular layer. All layer groups were significantly different from each other. SOM cells are expressed in all layers, except Layer I (Riedemann, 2019). This study found SOM cells in Layers II-VI, but mostly in the infragranular layers. Again, all layer groups were significantly different from each other.

This study found α2nAChR subunit expressed primarily in infragranular layers of ACx versus granular or supragranular layers. These findings are in line with Hilscher et al., (2017), where 97.6% α2nAChR cells were found in LV of A1. We found that 52.7% of α2nAChR subunits were colocalized with SOM, which is high compared to 30.3% in Hilscher et al., (2017). However, that study focused on A1, and we considered all of ACx. Colocalization of α2nAChR with PV and VIP markers was negligible.

Considering that PV, VIP, and SOM-expressing cells make up 82% of all GABAergic interneurons, it is curious that nearly half of α2-expressing cells did not colocalize with either of these cell types. There were no sex differences in laminar distribution, expression, or colocalization for any of the markers studied. This is the first time α2nAChR subunit colocalization with PV, VIP, or SOM cells has been characterized within in ACx.

GENERAL DISCUSSION

Nicotine acts on nAChRs, to improve sensory-cognitive function, learning, and memory -- likely through enhanced neurophysiology (Mansvelder et al., 2006; Lawrence et al., 2002; Dani and Bertrand, 2007; Newhouse P et al., 2012). Conversely, compromised nAChR activation (e.g., genetic deletion, disease-induced) impedes sensory processing and cognition, resulting in diminished performance on sensory and memory related tasks (Warburton, 1992; Levin et al., 2006). Accordingly, nicotine and other nAChR agonists are regarded as possible therapies for people with impaired cognition due to, for example, ADHD, Alzheimer's, and schizophrenia (Potter and Newhouse, 2008; Levin et al., 2006; Newhouse PA et al., 2004; Newhouse P et al., 2012). While this idea is promising, our restricted understanding of diverse nAChR compositions and how their respective functions integrate into neurocircuitry is a limiting factor in developing effective therapeutics. A necessary step in working toward that goal is discerning the roles of specific nAChR subtypes in cortical and subcortical sensory processing. It will also require increasing our knowledge of their laminar expression as well as specific cell types where they can be found.

Subcortically, nAChRs may be involved in mediating the amplification of bottom-up sensory information to cortical regions (Kawai et al., 2007; Mukherjee et al., 2018; Askew et al., 2017). Within the cortex, nAChRs are found in both excitatory and inhibitory neurons (Poorthuis et al., 2013; Kawai et al., 2007; Gil et al., 1997; Aracri et al., 2010), where they help modulate thalamocortical signals and intracortical processing (Metherate et al., 2005; Intskirveli and Metherate, 2012). These mechanisms can be

influenced differentially based on nAChRs expression on neuronal types, and membrane domains, as well as their laminar distribution and desensitization properties.

We investigated the α2nAChR as a potentially important contributor to auditory-cognitive function, using *in-vivo* electrophysiology in mouse A1 and conducted immunohistochemistry experiments to identify its expression within the neuronal circuitry of mouse ACx.

α2nAChR subunit and A1 processing of pure tone stimuli

Systemic nicotine enhances A1 responses to pure tone stimuli, in that response onset latency is reduced, and response slope and amplitude increase. In this study, deletion of the α2nAChR subunit resulted in no nicotinic enhancement of onset latency and attenuated enhancement of initial slope, significantly smaller than that of WT animals (Figures 9 and 10). However, the nicotinic enhancement of 5ms and 20ms amplitude of A1 responses remained (Figures 11 and 12). Onset latency and initial slope reflect thalamocortical input and response amplitude at 5ms and 20ms reflects increasing amounts of intracortical activity (Intskirveli et al., 2016; Metherate et al., 2015). Therefore, our results suggest that the nicotinic enhancement of onset/initial slope and later amplitudes are mediated differentially. Specifically, nicotinic enhancement of response onset and initial slope involve subcortical α2nAChR activation, and enhancement of response amplitude is mediated by other means.

Although, to our knowledge, there is currently no published information on subcortical α2nAChR subunit expression in the ascending auditory pathway, Wada et al., (1989) found α2nAChR subunit mRNA in the superior olive, lateral lemniscus, and

inferior colliculi. The lateral lemniscus is the portion of the brainstem auditory tract that connects SOC and IC (Figure 1). Moreover, IC send projections the medial geniculate nuclei (MGN), and Han et al., (2000) found α2nAChR subunit mRNA in Rhesus monkey MGN, which has direct projections to A1.

Also highly relevant to this particular study, in imaged brain sections of Chrna2-EGFP mice, a substantial number of α2 processes are visible within the MGN in mice (unpublished observation, Metherate lab, 2021). Although there are no cell bodies of α2-expressing cells, this observation clearly indicates that α2nAChRs could regulate thalamocortical inputs to ACx. It is plausible that nicotinic activation of α2nAChRs in one or more subcortical region could result in the disinhibition of thalamic cells. More excitable thalamic cells could increase monosynaptic input to A1, resulting in a decreased onset latency and increased initial slope of the cortical response.

Future directions

Further experiments are needed to determine if the superior olive, lateral lemniscus, and inferior colliculi express α2nAChRs, as does the MGN. Knowing which subcortical structures contain α2nAChRs would allow the region-specific silencing of these receptors, which would help identify which α2-expressing region(s) is/are involved in producing our current results. Designer receptors exclusively activated by designer drugs (DREADDs) and/or optogenetics to alternatively silence IC/SOC could be used, while recording (in-vitro) within ACx to identify if α2nAChR expression in IC and/or SOC is sufficient and/or necessary for nicotinic enhancement of OL and slope.

However, the question of cortical α2nAChR function still remains. Because this

study found that 52.7% of α2nAChR subunit expression in ACx is in SOM-expressing cells, it is important to investigate the cortical function of this population. SOM-expressing interneurons are largely MCs, whose axons have ascending translaminar axon collaterals which arborize in Layers I and III. Analyzing responses in supragranular layers would be an excellent way to continue investigating whether cortical α2nAChRs contribute to nicotinic enhancement of responses in more superficial layers.

Analyzing responses in Layer V might also lead to interesting questions regarding the possibility of α2nAChRs influencing A1 output, as MC axons also have dense local ramifications. Layer V is considered to be the main output layer of the cortex (Constantinople and Bruno, 2013); and our study found α2nAChRs expression mainly in Layer V.

Additionally, a study by Weedman and Ryugo, (1996) found that descending projections from Layer V PCs provide direct and exclusive innervation of neurons within CN and SOC (both part of the ascending auditory pathway). If Layer V α2nAChR-expressing cells modulate Layer V-output PCs, then these receptors could have a direct effect on the processing of auditory information coming from these regions (CN and SOC).

Colocalization of α2 subunit with VIP+, PV+ or SOM+

The focus of this project was to expand what is currently known about α2nAChR expression within ACx. To this end, after brain tissue was sectioned stained and imaged, I measured the laminar expression of α2nAChR subunit, PV, VIP, and SOM, as well as the colocalization of α2nAChR with the above three interneuron types.

Our results found: PV expression throughout laminae, but predominantly in infragranular layers and least in granular layer; the highest expression of VIP cells in supragranular layers, and the lowest in granular layer; and SOM expression in all layers except Layer I, with the most expression in infragranular layers. Our findings were in line with Rudy et al., (2011) and Riedemann, (2019). For each marker, all layers were significantly different from each other, and there were no laminar distribution or expression differences across sex.

We also found that α2nAChR subunit is expressed primarily in infragranular layers of ACx. This is in line with Hilscher et al., (2017), where 97.6% α2nAChR cells were found in LV of A1. These results suggest that α2nAChR subunits play a layer-specific role within ACx, possibly involving top-down processing, as Layer V is the major output layer of A1.

In this study, 52.7% of α2nAChR subunits were colocalized with SOM. This is high compared to 30.3% (all layers) in Hilscher et al., (2017). Notably, colocalization of α2nAChR with PV and VIP was negligible. Considering that PV, VIP, and SOM-expressing cells make up 82% of all GABAergic interneurons, it is curious that nearly half of α2nAChRs were not localized within either of these cell types.

As far as we are aware, this the first time α2nAChR subunit expression and colocalization with PV, VIP, and SOM cells have been characterized within in A1.

Future direction

We found 52.7% α2nAChRs localized within SOM-expressing cells, meaning we still don't know which type of cells express the other 47.3%. Using single-cell reverse

56

transcription, Hilscher et al., (2017) determined that 85.7% of cells tested were inhibitory in nature. Therefore, in trying to identify cell types for the remaining population of α2nAChRs, it makes sense to continue exploring interneurons. This study focused on PV, VIP, and SOM interneurons, which account for roughly 82% of all interneurons (Rudy et al., 2011). Presumably, the remaining 18% comprise the non-VIP subclass of 5HT3aR-expressing interneurons. While VIP interneurons make up 40% of the 5HT3aR interneuron class, the other 60% does not express VIP and would not have been immunolabeled in this experiment. Of these unlabeled neurons, 80% express Reelin. However, Reelin-expressing cells are mainly in Layer I, and our findings show α2nAChRs mainly in Layer V. Additionally, Ramos-Moreno and Clasca, (2013), show that the main source of Reelin in Layer I comes from Martinotti cells, which also express SOM. The other 20% of the non-VIP subclass do not have known markers. Therefore, the lack of markers for 5HT3aR/non-VIP interneurons precludes the use of antibodies to further characterize α2nAChR expression within ACx.

A feasible next-step is to presume that the α2-expressing cells we found localized within SOM interneurons are, as with Hilscher et al., (2017), Martinotti cells. Their research found that Layer V MCs are connected primarily to Type-A PCs (TAPC), which are known as subcortical projection (pyramidal tract) neurons (Hilscher et al., 2017). These observations could correspond to the possibility raised in Chapter 1 *Future directions*. Specifically, α2nAChR-expressing cells could influence Layer V output to SOC and CN, which could (indirectly) influence input to A1.

To test this, retrograde tracers injected into various regions of CN (Schofield et al., 2006) and SOC (Riemann and Reuss, 1998) would reveal Layer V PCs projecting to those nuclei. Patching pairs of these PCs and neighboring α2eGFP-expressing cells be identified, and PCs could be filled with biocytin. Afterward sections could be stained for biocytin and immunolabeled for SOM expression to examine whether PCs innervating SOC and CN are TAPCs that are connected to MCs.

If so, it would follow that deletion of α2nAChR would eliminate the nicotinic enhancement of that connection, affecting both direct output and indirect input to A1. If the effect were an attenuation of signal from subcortical structures, considering that traces in our physiology experiment averaged 25 presentations of pure tone within each block, later presentations could have shorter onsets in WT animals but remain the same in KO (no nicotinic enhancement).

The outcome of the individual proposed future experiments will expand what we currently know about α2nAChRs. The studies discussed here would extend our understanding of the neural circuitry surrounding α2nAChRs within cortex and subcortically, both of which are necessary for understanding their respective role and function. The more thorough our understanding of each nAChR subtype, the better we can help inform the development of therapeutics that target cognitive disorders.

REFERENCES

Albuquerque EX, Pereira EF, Alkondon M, Rogers SW. Mammalian nicotinic acetylcholine receptors: from structure to function. *Physiol Rev*. 2009; 89(1):73–120.

Anderson LA, Christianson GB, Linden JF. Mouse auditory cortex differs from visual and somatosensory cortices in the laminar distribution of cytochrome oxidase and acetylcholinesterase. *Brain Res*. 2009; 1252:130-142. doi:10.1016/j.brainres.2008.11.037

Aracri, P, Consonni, S, Morini, R, Perrella, M, Rodighiero, S, Amadeo, Alida, and Becchetti, A. Tonic modulation of GABA release by nicotinic acetylcholine receptors in layer V of the murine prefrontal cortex. *Cereb. Cortex*. 2010; 20: 1529-1555.

Arendash GW, Sanberg PR, Sengstock GJ. Nicotine enhances the learning and memory of aged rats. *Pharmacol Biochem Behav*. 1995; 52(3):517–523.

Armbruster, B.N., Li, X., Pausch, M.H., Herlitze, S., Roth, B.L. Evolving the lock to fit the key to create a family of G protein-coupled receptors potently activated by an inert ligand. *Proceedings of the National Academy of Sciences.* 2007; 104(12): 5163–5168. doi:

Askew, C., Intskirveli, I. & Metherate, R. Systemic Nicotine Increases Gain and Narrows Receptive Fields in A1 via Integrated Cortical and Subcortical Actions. *eNeuro*. 2017; 4. pmcid: PMC5480142

Atasoy D, Aponte Y, Su HH, Sternson SM. A FLEX switch targets Channelrhodopsin-2 to multiple cell types for imaging and long-range circuit mapping. *J Neurosci*. 2008; 28(28):7025–7030. [PubMed: 18614669]

Cain SM, Snutch TP. T-type calcium channels in burst-firing, network synchrony, and epilepsy. *Biochim Biophys Acta*. 2013;1828(7):1572-1578. doi:10.1016/j.bbamem.2012.07.028

Calford MB, Webster WR, Semple MM. Measurement of frequency selectivity of single neurons in the central auditory pathway. *Hear Res*. 1983; 11(3):395–401.

Carter ME, Soden ME, Zweifel LS, Palmiter RD. Genetic identification of a neural circuit that suppresses appetite. *Nature*. 2013; 503(7474):111–114. [PubMed: 24121436]

Constantinople CM, Bruno RM. Deep cortical layers are activated directly by thalamus *Science*. 2013;340(6140):1591-1594. doi:10.1126/science.1236425

Crooks PA, Bardo MT, Dwoskin LP. Nicotinic receptor antagonists as treatments for nicotine abuse. *Adv Pharmacol*. 2014; 69:513–551.

Cruikshank, S.J., Rose, H.J., and Metherate, R. Auditory Thalamocortical Synaptic Transmission In Vitro. *Journal of Neurophysiology.* 2001; 87: 361–384, 2002; 10.1152/jn.00549.2001.

Dani JA, Bertrand D. Nicotinic acetylcholine receptors and nicotinic cholinergic mechanisms of the central nervous system. *Annual Review Pharmacology*

Toxicology. 2007; 47:699–729.

Evans, D.E. & Drobes, D.J. Nicotine self-medication of cognitive-attentional processing. *Addiction Biology*. 2009; 14, 32-42. pmcid:

Férézou I, Cauli B, Hill EL, Rossier J, Hamel E, Lambolez B. 5-HT3 receptors mediate serotonergic fast synaptic excitation of neocortical vasoactive intestinal peptide/cholecystokinin interneurons. *J Neurosci*. 2002;22(17):7389-7397. doi:10.1523/JNEUROSCI.22-17-07389.2002

French KL, Granholm AC, Moore AB, Nelson ME, Bimonte-Nelson HA. Chronic nicotine improves working and reference memory performance and reduces hippocampal NGF in aged female rats. *Behav Brain Res*. 2006;169(2):256–262.

Friedman, J., Horvath, T. & Meares, R. Tobacco smoking and a 'stimulus barrier'. *Nature*. 1974; 248, 455-456. pmcid:

Gil Z, Connors BW, Amitai Y. Differential regulation of neocortical synapses by neuromodulators and activity. *Neuron*. 1997; 19(3):679–686.

Girod R, Barazangi N, McGehee D, Role LW. Facilitation of glutamatergic neurotransmission by presynaptic nicotinic acetylcholine receptors. *Neuropharmacology*. 2000; 39(13):2715–2725.

Gold M, Newhouse PA, Howard D, Kryscio RJ. Nicotine treatment of mild cognitive impairment: a 6-month double-blind pilot clinical trial. *Neurology*. 2012; 78(23):1895; author reply 1895.

Goldberg EM, Coulter DA. Mechanisms of epileptogenesis: a convergence on neural circuit dysfunction. *Nat Rev Neurosci*. 2013;14(5):337-349. doi:10.1038/nrn3482

Gotti C, Moretti M, Bohr I, et al. Selective nicotinic acetylcholine receptor subunit deficits identified in Alzheimer's disease, Parkinson's disease and dementia with Lewy bodies by immunoprecipitation. *Neurobiol Dis*. 2006; 23(2):481–489.

Griguoli M, Cherubini E. Regulation of hippocampal inhibitory circuits by nicotinic acetylcholine receptors. *J Physiol*. 2012;590(4):655-666. doi:10.1113/jphysiol.2011.220095

Grilly DM. A verification of psychostimulant-induced improvement in sustained attention in rats: effects of d-amphetamine, nicotine, and pemoline. *Experimental Clinical Psychopharmacology*. 2000; 8(1):14–21.

Han, Z.Y., N. Le Novere, M. Zoli, J.A. Hill, Jr., N. Champtiaux, and J.P. Changeux, *Localization of nAChR subunit mRNAs in the brain of Macaca mulatta. Eur J Neurosci*. 2000; 12(10): p. 3664-74.

Hara K, Harris RA. The anesthetic mechanism of urethane: the effects on neurotransmitter-gated ion channels. *Anesth Analg*. 2002;94(2): doi:10.1097/00000539-200202000-00015

Hilscher MM, Leão RN, Edwards SJ, Leão KE, Kullander K. Chrna2-Martinotti Cells Synchronize Layer 5 Type A Pyramidal Cells via Rebound Excitation. *PLoS Biol*. 2017;15(2): e2001392. Published 2017 Feb 9. doi:10.1371/journal.pbio.2001392

Horst, N.K., Heath, C.J., Neugebauer, N.M., Kimchi, E.Y., Laubach, M. & Picciotto, M.R. Impaired auditory discrimination learning following perinatal nicotine exposure or β2 nicotinic acetylcholine receptor subunit deletion. *Behavioural Brain Research*. 2012; 231, 170-180. pmcid:

Hu H, Gan J, Jonas P. Interneurons. Fast-spiking, parvalbumin⁺ GABAergic interneurons: from cellular design to microcircuit function. *Science*. 2014;345(6196):1255263. doi:10.1126/science.1255263

Hughes JR, Pillitteri JL, Callas PW, Callahan R, Kenny M. Misuse of and dependence on over-the-counter nicotine gum in a volunteer sample. *Nicotine Tobacco Res*earch 2004; 6(1):79–84.

Intskirveli, I. & Metherate, R. Nicotinic neuromodulation in auditory cortex requires MAPK activation in thalamocortical and intracortical circuits. *J Neurophysiol*. 2012; 107, 2782-2793. pmcid: 3362282

Jia Y, Yamazaki Y, Nakauchi S, Sumikawa K. Alpha2 nicotine receptors function as a molecular switch to continuously excite a subset of interneurons in rat hippocampal circuits. *Eur J Neurosci*. 2009; 29(8):1588–1603.

Jiang X, Shen S, Cadwell CR, et al. Principles of connectivity among morphologically defined cell types in adult neocortex. *Science*. 2015;350(6264):aac9462. doi:10.1126/science.aac9462

Kassel, J.D. Smoking and attention: a review and reformulation of the stimulus-filter hypothesis. *Clin Psychol Rev*. 1997; 17, 451-478. pmcid:

Kaur S, Lazar R, Metherate R. Intracortical pathways determine breadth of subthreshold frequency receptive fields in primary auditory cortex. *J Neurophysiol*. 2004; 91(6):2551–2567.

Kawai, H.D., Kang, H.A. & Metherate, R. Heightened nicotinic regulation of auditory cortex during adolescence. *J Neurosci*. 2011; 31, 14367-14377. pmcid: 3210642

Kawai, H.D., La, M., Kang, H, Hashimoto, Y., Liang, K., Lazar, R., and Metherate, R. Convergence of nicotine-induced and auditory-evoked neural activity activates ERK in auditory cortex. *Synapse*. 2013; 67(8): 455–468. doi:10.1002/syn.21647.

Kawai H, Lazar R, Metherate R. Nicotinic control of axon excitability regulates thalamocortical transmission. *Nat Neurosci*. 2007;10(9):1168–1175.

Kleeman E, Nakauchi S, Su H, Dang R, Wood MA, Sumikawa K. Impaired function of α2-containing nicotinic acetylcholine receptors on oriens-lacunosum moleculare cells causes hippocampus-dependent memory impairments. *Neurobiol Learn Mem*. 2016; 136:13–20.

Knott, V.J., Bolton, K., Heenan, A., Shah, D., Fisher, D.J. & Villeneuve, C. Effects of acute nicotine on event-related potential and performance indices of auditory distraction in nonsmokers. Nicotine Tobacco Research. 2009; 11, 519-530. pmcid:

Lakatos P, Musacchia G, O'Connel MN, Falchier AY, Javitt DC, Schroeder CE. The spectrotemporal lter mechanism of auditory selective attention. *Neuron*. 2013; 77(4):750–761.

Lawrence NS, Ross TJ, Stein EA. Cognitive mechanisms of nicotine on visual attention. *Neuron*. 2002;36(3):539-548. doi:10.1016/s0896-6273(02)01004-8

Leão RN, Mikulovic S, Leão KE, et al. OLM interneurons differentially modulate CA3 and entorhinal inputs to hippocampal CA1 neurons. *Nat Neurosci*. 2012; 15(11):1524–1530.

Levin, E.D., McClernon, F.J. & Rezvani, A.H. Nicotinic effects on cognitive function: behavioral characterization, pharmacological specification, and anatomic localization. Psychopharmacology (Berl). 2006; 184, 523-539. pmcid:

Lotfipour S, Mojica C, Nakauchi S, et al. α2* Nicotinic acetylcholine receptors influence hippocampus-dependent learning and memory in adolescent mice. *Learn Mem*. 2017; 24(6):231–244.

Mao, B. Q., MacLeish, P. R., & Victor, J. D. (2003). Role of hyperpolarization-activated currents for the intrinsic dynamics of isolated retinal neurons. *Biophysical journal*, *84*(4), 2756–2767. https://doi.org/10.1016/S0006-3495(03)75080-2

Mao, D., Perry, D.C., Yasuda, R.P., Wolfe, B.B. & Kellar, K.J. The alpha4beta2alpha5 nicotinic cholinergic receptor in rat brain is resistant to up-regulation by nicotine in vivo. *J Neurochem*. 2008; 104, 446-456. pmcid:

Mansvelder HD, van Aerde KI, Couey JJ, Brussaard AB. Nicotinic modulation of neuronal networks: from receptors to cognition. *Psychopharmacology (Berl)*. 2006; 184(3–4):292–305.

Marín O. Interneuron dysfunction in psychiatric disorders. *Nat Rev Neurosci*. 2012;13(2):107-120. Published 2012 Jan 18. doi:10.1038/nrn3155

Mazzaferro S, Bermudez I, Sine SM. α4β2 Nicotinic acetylcholine receptors: relationships between subunit stoichiometry and function at the single channel level. *J Biol Chem*. 2017; 292(7):2729–2740.

McGehee DS, Heath MJ, Gelber S, Devay P, Role LW. Nicotine enhancement of fast excitatory synaptic transmission in CNS by presynaptic receptors. *Science*. 1995; 269(5231):1692–1696.

Metherate R, Kaur S, Kawai H, Lazar R, Liang K, Rose HJ. Spectral integration in auditory cortex: mechanisms and modulation. *Hear Res*. 2005; 206(1–2):146–158.

Milton NG, Bessis A, Changeux JP, Latchman DS. The neuronal nicotinic acetylcholine receptor alpha 2 subunit gene promoter is activated by the Brn-3b POU family transcription factor and not by Brn-3a or Brn-3c. *J Biol Chem*. 1995;270(25):15143-15147. doi:10.1074/jbc.270.25.15143

Moore AK, Wehr M. Parvalbumin-expressing inhibitory interneurons in auditory cortex are well-tuned for frequency. *J Neurosci*. 2013;33(34):13713-13723. doi:10.1523/JNEUROSCI.0663-13.2013

Mukherjee J, Lao PJ, Betthauser TJ, et al. Human brain imaging of nicotinic acetylcholine α4β2* receptors using [18 F]Nifene: selectivity, functional activity, toxicity, aging effects, gender effects, and extrathalamic pathways. *J Comp Neurol*. 2018; 526(1):80–95.

Müller-Preuss P, Mitzdorf U. Functional anatomy of the inferior colliculus and the auditory cortex: current source density analyses of click-evoked potentials. *Hear Res*. 1984;16(2):133-142. doi:10.1016/0378-5955(84)90003-0

Nakauchi S, Brennan RJ, Boulter J, Sumikawa K. Nicotine gates long-term potentiation in the hippocampal CA1 region via the activation of alpha2* nicotinic ACh receptors. *Eur J Neurosci*. 2007; 25(9): 2666–2681.

Newhouse P, Kellar K, Aisen P, et al. Nicotine treatment of mild

cognitive impairment: a 6-month double-blind pilot clinical trial. *Neurology*. 2012; 78(2):91–101.

Newhouse PA, Potter A, Singh A. Effects of nicotinic stimulation on cognitive performance. *Curr Opin Pharmacol*. 2004; 4(1):36–46.

Newman E. L., Gupta K., Climer J.R., Monaghan C.K., and Hasselmo M.E. Cholinergic modulation of cognitive processing: insights drawn from computational models. *Behavioral Neuroscience*. 2012; doi: 10.3389/fnbeh.2012.00024

O'Connell MN, Barczak A, Schroeder CE, Lakatos P. Layer specific sharpening of frequency tuning by selective attention in primary auditory cortex. *J Neurosci*. 2014; 34(49):16496–16508.

Okamoto H, Stracke H, Wolters CH, Schmael F, Pantev C. Attention improves population-level frequency tuning in human auditory cortex. *J Neurosci*. 2007; 27(39):10383–10390.

Ortells MO, Barrantes GE. Tobacco addiction: a biochemical model of nicotine dependence. *Med Hypotheses*. 2010; 74(5):884–894.

Packer AM, Yuste R. Dense, unspecific connectivity of neocortical parvalbumin-positive interneurons: a canonical microcircuit for inhibition. *J Neurosci*. 2011; 31(37):13260-13271. doi:10.1523/JNEUROSCI.3131-11.2011

Patterson, RD, Hackney, CM, Iversen, SD. Interdisciplinary auditory neuroscience. *TiCS*. 1999; 3 (7):245-247. doi.org/10.1016/S1364-6613(99)01347-9

Pi HJ, Hangya B, Kvitsiani D, Sanders JI, Huang ZJ, Kepecs A. Cortical interneurons that specialize in disinhibitory control. *Nature*. 2013; 503(7477):521–524.

Picciotto MR, Zoli M, Changeux JP. Use of knock-out mice to determine the molecular basis for the actions of nicotine. *Nicotine Tob Res*. 1999;1 Suppl 2: S121-S140. doi:10.1080/14622299050011931

Pickles, J.O. Chapter 1 - Auditory pathways: anatomy and physiology. *Handbook of Clinical Neurology*. 2015; 129 (3-25).

Poorthuis RB, Bloem B, Schak B, Wester J, de Kock CP, Mansvelder HD. Layer-specific modulation of the prefrontal cortex by nicotinic acetylcholine receptors. *Cereb Cortex*. 2013; 23(1):148–161.

Porter JT, Cauli B, Staiger JF, Lambolez B, Rossier J, Audinat E. Properties of bipolar VIPergic interneurons and their excitation by pyramidal neurons in the rat neocortex. *Eur J Neurosci*. 1998;10(12):3617-3628. doi:10.1046/j.1460-9568.1998.00367.x

Porter JT, Cauli B, Tsuzuki K, Lambolez B, Rossier J, Audinat E. Selective excitation of subtypes of neocortical interneurons by nicotinic receptors. *J Neurosci*. 1999; 19(13):5228–5235.

Potter AS, Newhouse PA. Acute nicotine improves cognitive deficits in young adults with attention-deficit/hyperactivity disorder. *Pharmacology Biochemistry Behavior*. 2008; 88(4):407–417.

Ramos-Moreno T, Clascá F. Quantitative mapping of the local and extrinsic sources of GABA and Reelin to the layer Ia neuropil in the adult rat neocortex. *Brain Struct Funct*. 2014;219(5):1639-1657. doi:10.1007/s00429-013-0591-x

Riedemann T. Diversity and Function of Somatostatin-Expressing Interneurons in the Cerebral Cortex. *Int J Mol Sci*. 2019;20(12):2952. Published 2019 Jun 17. doi:10.3390/ijms20122952

Riekkinen M, Riekkinen P Jr. Nicotine and D-cycloserine enhance acquisition of water maze spatial navigation in aged rats. *Neuroreport*. 1997; 8(3):699–703.

Riemann R, Reuss S. Projection neurons in the superior olivary complex of the rat auditory brainstem: a double retrograde tracing study. *ORL J Otorhinolaryngol Relat Spec*. 1998;60(5):278-282. doi:10.1159/000027610

Rudy B, Fishell G, Lee S, Hjerling-Leffler J. Three groups of interneurons account for nearly 100% of neocortical GABAergic neurons. *Dev Neurobiol*. 2011;71(1):45-61. doi:10.1002/dneu.20853

Said SI, Mutt V. Polypeptide with broad biological activity: isolation from small intestine. *Science*. 1970;169(3951):1217-1218. doi:10.1126/science.169.3951.1217

Sarter, M., Parikh, V. & Howe, W.M. nAChR agonist-induced cognition enhancement: integration of cognitive and neuronal mechanisms. *Biochem Pharmacol*. 2009; 78, 658-667. pmcid:

Scheyltjens I, Arckens L. The Current Status of Somatostatin-Interneurons in Inhibitory Control of Brain Function and Plasticity. *Neural Plast*. 2016; 2016:8723623. doi:10.1155/2016/8723623

Schofield BR, Coomes DL, Schofield RM. Cells in auditory cortex that project to the cochlear nucleus in guinea pigs. *J Assoc Res Otolaryngol*. 2006;7(2):95-109. doi:10.1007/s10162-005-0025-4

Shigematsu N, Nishi A, Fukuda T. Gap Junctions Interconnect Different Subtypes of Parvalbumin-positive interneurons in barrels and septa with connectivity unique to each subtype. *Cereb. Cortex*. 2019;29(4):1414-1429. doi:10.1093/cercor/bhy038

Socci DJ, Sanberg PR, Arendash GW. Nicotine enhances Morris water maze performance of young and aged rats. *Neurobiol Aging*. 1995; 16(5):857–860.

Stachniak, T.J., Ghosh, A., Sternson, S.M. Chemogenetic synaptic silencing of neural circuits localizes a hypothalamus→midbrain pathway for feeding behavior. *Neuron* 2014; 82(4): 797–808.

Stiebler, I, Neulist, R, Fichtel, I, Ehret, G. The auditory cortex of the house mouse: left-right differences, tonotopic organization and quantitative analysis of frequency representation. *Journal of Comparative Physiology*. 1997; 181(6):559-71.

Szymanski, F, Garcia-Lazaro, J, Schnupp. Current source density profiles of stimulus-specific adaptation in rat auditory cortex. *J. Neurophysio*l. 2009; 102: 1483-90. doi:10.1152/jn.00240.2009.

Takesian AE, Bogart LJ, Lichtman JW, Hensch TK. Inhibitory circuit gating of auditory critical-period plasticity. *Nat Neurosci*. 2018;21(2):218–227. 28. Newhouse PA, Potter A, Singh A. Effects of nicotinic stimulation on cognitive performance. *Curr Opin Pharmacol*. 2004; 4(1):36–46.

Taly A, Corringer PJ, Guedin D, Lestage P, Changeux JP. Nicotinic receptors: allosteric transitions and therapeutic targets in the nervous system. *National Rev Drug Discovery*. 2009; 8(9):733–750.

Tassonyi E, Charpantier E, Muller D, Dumont L, Bertrand D. The role of nicotinic acetylcholine receptors in the mechanisms of anesthesia. *Brain Res Bull*. 2002;57(2):133-150. doi:10.1016/s0361-9230(01)00740-7

Terry, A.V., Jr., Buccafusco, J.J., Jackson, W.J., Zagrodnik, S., Evans-Martin, F.F. & Decker, M.W. Effects of stimulation or blockade of central nicotinic-cholinergic receptors on performance of a novel version of the rat stimulus discrimination task. Psychopharmacology (Berl). 1996; 123, 172-181. pmcid:

Timofeeva, Y., Coombes, S. & Michieletto, D. Gap Junctions, Dendrites and Resonances: A Recipe for Tuning Network Dynamics. *J. Math. Neurosc.* **3,** 15 (2013). https://doi.org/10.1186/2190-8567-3-15

Tremblay R, Lee S, Rudy B. GABAergic Interneurons in the Neocortex: From Cellular Properties to Circuits. *Neuron*. 2016;91(2):260-292. doi:10.1016/j.neuron.2016.06.033

Trimmel M, Wittberger S. Effects of transdermally administered nicotine on aspects of attention, task load, and mood in women and men. *Pharmacology Biochemistry Behavior*. 2004; 78(3):639–645.

Volk DW, Lewis DA. Early developmental disturbances of cortical inhibitory neurons: contribution to cognitive deficits in schizophrenia. *Schizophr Bull*. 2014;40(5):952-957. doi:10.1093/schbul/sbu111

Wada E, Wada K, Boulter J, et al. Distribution of alpha 2, alpha 3, alpha 4, and beta 2 neuronal nicotinic receptor subunit mRNAs in the central nervous system: a hybridization histochemical study in the rat. *J Comp Neurol*. 1989; 284(2):314–335.

Wada K, Ballivet M, Boulter J, et al. Functional expression of a new pharmacological subtype of brain nicotinic acetylcholine receptor. *Science*. 1988; 240(4850):330–334.

Warburton, D.M. Nicotine as a cognitive enhancer. Prog Neuropsychopharmacol Biol Psychiatry. 1992; 16, 181-191. pmcid:

Weedman DL, Ryugo DK. Pyramidal cells in primary auditory cortex project to cochlear nucleus in rat. *Brain Res*. 1996;706(1):97-102. doi:10.1016/0006-8993(95)01201-x

Wenk GL. The nucleus basalis magnocellularis cholinergic system: one hundred years of progress. *Neurobiol Learn Mem*. 1997; 67(2):85–95.

Whiteaker P, Wilking JA, Brown RW, et al. Pharmacological and immunochemical characterization of alpha2* nicotinic acetylcholine receptors (nAChRs) in mouse brain. *Acta Pharmacol Sin*. 2009; 30(6):795–804.

Wu, C., Stefanescu, R.A., Martel D.T., and Shore, S.E. Listening to another sense: somatosensory integration in the auditory system. Cell Tissue Res. 2015; 361(1): 233–250. doi:10.1007/s00441-014-2074-7.

Xiao Y, Kellar KJ. The comparative pharmacology and up-regulation of rat neuronal

nicotinic receptor subtype binding sites stably expressed in transfected mammalian cells. *J Pharmacol Exp Ther*. 2004; 310(1):98–107.

Xu X, Callaway EM. Laminar specificity of functional input to distinct types of inhibitory cortical neurons. *J Neurosci*. 2009;29(1):70-85. doi:10.1523/JNEUROSCI.4104-08.2009